Citation: Seyitoğlu, G., Aktuğ, B., Esat, K., Kaypak, B., 2022. Neotectonics of Turkey (Türkiye) and surrounding regions: a new perspective with block modelling. Geologica Acta, 20.4, 1-21.
DOI: 10.1344/GeologicaActa2022.20.4

geologica acta

Neotectonics of Turkey (Türkiye) and surrounding regions: a new perspective with block modelling

Gürol Seyitoğlu[1] Bahadır Aktuğ[2] Korhan Esat[1] Bülent Kaypak[2]

[1]Department of Geological Engineering, Tectonics Research Group, Ankara University
06830 Ankara, Turkey. E-Mail: seyitoglu@ankara.edu.tr; esat@ankara.edu.tr

[2]Department of Geophysical Engineering, Ankara University
06830 Ankara, Turkey. E-Mail: aktug@ankara.edu.tr; kaypak@eng.ankara.edu.tr

ABSTRACT

This paper aims to present a new neotectonic perspective concordant with the seismic activities in Turkey and surrounding regions. The neotectonic structures have been re-evaluated mainly by using focal mechanism solutions and high-resolution satellite (Google Earth) images. The Southeast Anatolian Wedge explains thrust/blind thrust and asymmetrical folding relationship in SE Turkey, Syria, and Northern Iraq. The neotectonic structures of the Turkish-Iranian Plateau are enlightened by the rhomboidal cell model which creates a base to determine multiple intersection points between the region-wide left- and right-lateral shear zones. The releasing stepover between the North Anatolian Fault Zone and Southeast Anatolian-Zagros Fault Zone, plus their connections with the Northeast Anatolian Fault Zone and the East Anatolian Fault Zone are described in a more meaningful way with the Anatolian Diagonal concept. It also clarifies the role of left-lateral shear zone in the west-southwest movement of Anatolian plate and its relationship with the Aegean and Cyprus arcs. A neotectonic region under the influence of NW-SE contraction is determined between the North Anatolian, Eskişehir, and Kırıkkale-Erbaa fault zones in which the Elmadağ-Eldivan and Abdüsselam pinched crustal wedges and the Beypazarı Blind Thrust Zone are developed. A new route for the southern branch of the North Anatolian Fault Zone is determined between Bolu and Değirmenlik (Milos) Island in the Aegean Sea via Mudurnu, Bursa, Balıkesir, and İzmir. All main neotectonic structures mentioned in this paper are evaluated by the elastic dislocation modelling and new neotectonic provinces are suggested.

KEYWORDS **Neotectonics. Eastern Mediterranean. Turkish-Iranian Plateau. Earthquake. GNSS. Block modelling.**

INTRODUCTION

The initiation of neotectonic studies in Turkey can be attributed to the discovery of the North Anatolian Fault and the estimation of the East Anatolian Fault by Ketin (1948). Fundamentals of eastern Mediterranean neotectonics were established synchronously with the theory of plate tectonics. The plate boundaries around Turkey were recognized by using seismic activity and related focal mechanism solutions (McKenzie, 1972). The realization of plate movements and the nature of plate margins in eastern Mediterranean flourished the concept of tectonic escape model (Dewey and Şengör, 1979; Şengör, 1979; Şengör *et al.*, 1985).

This model establishes cause-effect relationships that explain the main neotectonic elements of Turkey. The

triggering event of this model is the collision of Arabian and Eurasian plates along the Bitlis-Zagros Suture Zone (BZSZ) between Late Maastrichtian and Late Miocene (Hall, 1976; Şengör and Kidd, 1979) that is believed to create a thickened crust in eastern Turkey (Dewey *et al.*, 1986). This thickened crust led to the formation of North and East Anatolian fault zones and the Anatolian plate moves westwards between these two strike-slip structures. The westward movement of Anatolian plate was prevented by the Grecian shear zone and consequently, N-S extension of western Turkey initiated in the Tortonian (Şengör, 1979; Şengör *et al.*, 1985).

The tectonic escape model briefly explained above allows defining the neotectonic provinces of Turkey such as East Anatolian Contractional, North Turkish, Central Anatolian "Ova" and West Anatolian Extensional provinces (Fig. 1A). Special structures are determined to explain the relationship between palaeo and neotectonic structures (*i.e.* resurrected, replacement, and revolutionary structures) (Şengör *et al.*, 1985) and a cross graben model has been proposed to explain age controversies from the sedimentary basins, especially in the West Anatolian Extensional Province (Şengör, 1987). For the time being, the active fault map of Şaroğlu *et al.* (1992a) was published and it carries some influences of the tectonic escape model such as the thrust component of Tuzgölü and Sultandağ faults (Fig. 1A).

The cause-effect relationship of the tectonic escape model has been questioned by using the latest Oligocene-Early Miocene initiation time of the "revolutionary structures" in western Turkey (Seyitoğlu and Scott, 1991, 1992, 1996a, b). Today, we have models that explain the causes and development process of extensional tectonics in the Aegean region with the formation of metamorphic core complexes (Bozkurt and Park, 1994; Emre and Sözbilir, 1997; Işık and Tekeli, 2001; Kamacı and Altunkaynak, 2019; Kurt *et al.*, 2010; Lister *et al.*, 1984; Ring *et al.*, 2003; Seyitoğlu *et al.*, 2004a; Seyitoğlu and Işık, 2015; Seyitoğlu and Esat, 2022).

Newly recognized fault zones and the increased number of focal mechanism solutions progressively provide additional information relative to the transition characteristics and internal deformation of the neotectonic provinces. Barka and Reilinger (1997), for example, attempted to revise the neotectonic framework of Turkey by suggesting that the Eskişehir Fault Zone and the Fethiye-Burdur Fault Zone separate western Turkey from central Anatolia and emphasized the existence of thrust faults along the Black Sea coast. The eastward movement of the Ahar block in the eastern Turkish-Iranian Plateau along with the Aras and Tebriz faults was also recognized (Barka and Reilinger, 1997) (Fig. 1B). An updated neotectonic map of Turkey was summarized by Bozkurt (2001).

The extensional nature of 2000.12.15 (Mw=6.0) Sultandağı and 2002.02.03 (Mw=6.5) Çay earthquakes changed the perception of neotectonic provinces. Koçyiğit and Özacar (2003) suggest that the extensional province in western Turkey can be extended to the Eskişehir and Tuzgölü fault zones (Fig. 1C).

The latest attempt to revise the neotectonic provinces was made by Emre *et al.* (2018) (Fig. 1D). Considering the West Anatolian Extensional Province, the neotectonic provinces defined by Emre *et al.* (2018) are somewhat similar to those of Koçyiğit and Özacar (2003). On the other hand, their newly introduced Southeast Anatolian Province differs from the approach of Şengör *et al.* (1985) and Koçyiğit and Özacar (2003) (Fig. 1D).

One fundamental step to define and discriminate neotectonic regions is the determination of the slip rates across faults and block boundaries. While direct field measurement of the fault offsets at fault trace provides invaluable information about the activity of the faults (Aksoy *et al.*, 2007; Arpat and Şaroğlu, 1972; Hempton, 1985), the local nature of this type of observations, their relatively low precision and the difficulty of its application at broader deformation zones makes them infeasible for full quantification of the slip rates. For a study at this scale covering the whole of Turkey and surrounding regions, no consistent set of geologic slip rates is available. Another popular method to determine the slip rates along block boundaries is the inversion of the observed Global Navigation Satellite Systems (GNSS) velocities using various numerical models (*e.g.* Aktuğ *et al.*, 2015; Aktuğ *et al.*, 2016; Reilinger *et al.*, 2006). In this approach, the observed annual motion at a GNSS site is modelled as the sum of block rigid rotation and the elastic strain along block boundaries. The slip rates across the faults are determined through the inversion of the observed GNSS velocities. There are several advantages of the geodetic determination of the slip rates such as its applicability over large areas, uncertainty modeling, inherently consistent kinematic model, determination of the slip rates from observations away from the fault traces, and the ability to model the slip rates even when no surface offsets are observable. Furthermore, it is also possible in this approach to test the consistency of the block slip rates with the observations.

In this study, a new block model of Turkey and surrounding regions is presented at an unprecedented scale and detail (1688 GNSS sites, 25 blocks). It should be noted that the block boundary discretization may not exactly follow the fault lineation, the block modeling still provides a first-order approximation of the slip rates due to

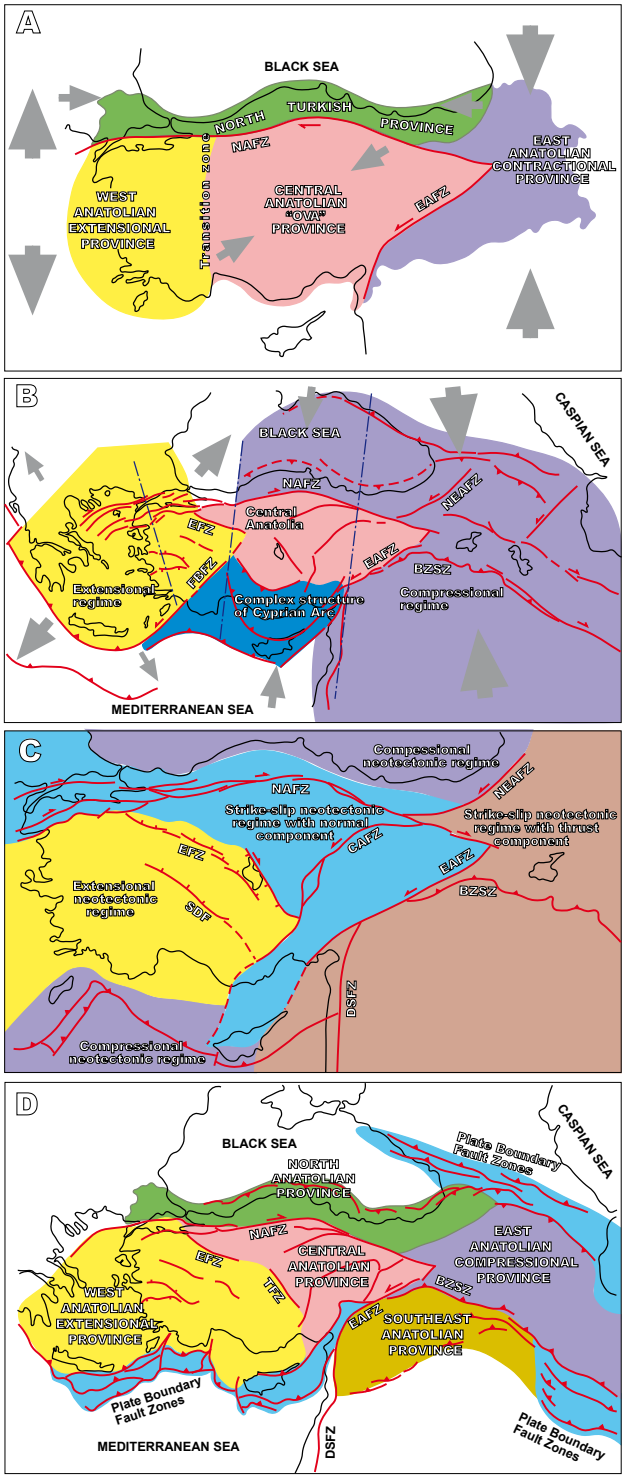

FIGURE 1. Neotectonic provinces of Turkey. A) Şengör *et al.* (1985)'s map. Grey arrows indicate contraction and extension directions. B) Barka and Reilinger (1997)'s compiled map. Dashed-dotted straight lines separate regions having different rates of extension or contraction. C) Koçyiğit and Özacar (2003)'s map. D) Emre *et al.* (2018)'s map. NAFZ: North Anatolian Fault Zone; EAFZ: East Anatolian Fault Zone; NEAFZ: Northeast Anatolian Fault Zone; BZSZ: Bitlis-Zagros Suture Zone; EFZ: Eskişehir Fault Zone; TFZ: Tuzgölü Fault Zone; SDF: Sultandağı Fault; FBFZ: Fethiye-Burdur Fault Zone; CAFZ: Central Anatolian Fault Zone; DSFZ: Dead Sea Fault Zone.

the relative motion between neighboring blocks. The results show that the proposed block model can model at least 90% of the slip rates considering that the Weighted Root Mean Squared (WRMS) is 2.1mm/yr with respect to the velocity magnitudes of the GNSS sites which range from 20 to 40mm/yr.

This paper aims to evaluate newly introduced structures as a whole, which are published as separate articles (Esat *et al.*, 2021; Seyitoğlu *et al.*, 2017a, 2018, 2022a, b), providing more reliable explanations for the seismic activities in the neotectonic provinces, such as Southeast Anatolian Wedge in SE Anatolia, rhomboidal cells in East Anatolia, the Anatolian Diagonal between east and central Anatolia, the Elmadağ-Eldivan, Abdüsselam pinched crustal wedges and Beypazarı Blind Thrust Zone in the NW Central Anatolia and the southern branch of NAFZ between Bolu and Değirmenlik (Milos) island. The motivation of this article is to improve the resolution of the current neotectonic zonation of the study region, that may help identifying earthquake-prone areas.

METHODS

The GNSS velocity field in the region provides an excellent quantification of the ongoing deformation and the variation of the slip rates along major fault zones. A subset of GNSS velocity observations covering the area of interest was extracted from the published velocity field given in (Kreemer *et al.*, 2014). The source GNSS velocity field in Kreemer *et al.* (2014) is actually a compilation of the published data sets which were rigorously transformed into a common reference frame (ITRF08).

In order to obtain the slip rate variations and how much of the observed motion comes from the rotation of the rigid blocks, a detailed block model covering the region is proposed. A block modeling approach (McCaffrey, 2002) was used to derive the slip rates across block boundaries. The employed methodology closely follows those given in (Aktuğ *et al.*, 2015, 2016). In order to account for the elastic strain accumulation near the block boundaries, the back-slip approach similar to that of McCaffrey (2002) is applied. In this scheme, the rotations of all the blocks in Euler parameterization are simultaneously estimated by minimizing the model misfit of the GNSS velocities. In the estimation of the block rotations, elastic back-slip is applied to each fault segment to mimic elastic strain accumulation during the interseismic phase of the earthquake cycle (Matsu'ura *et al.*, 1986). The effective elastic back-slip was computed through the elastostatic Green functions as given by Okada (1985).

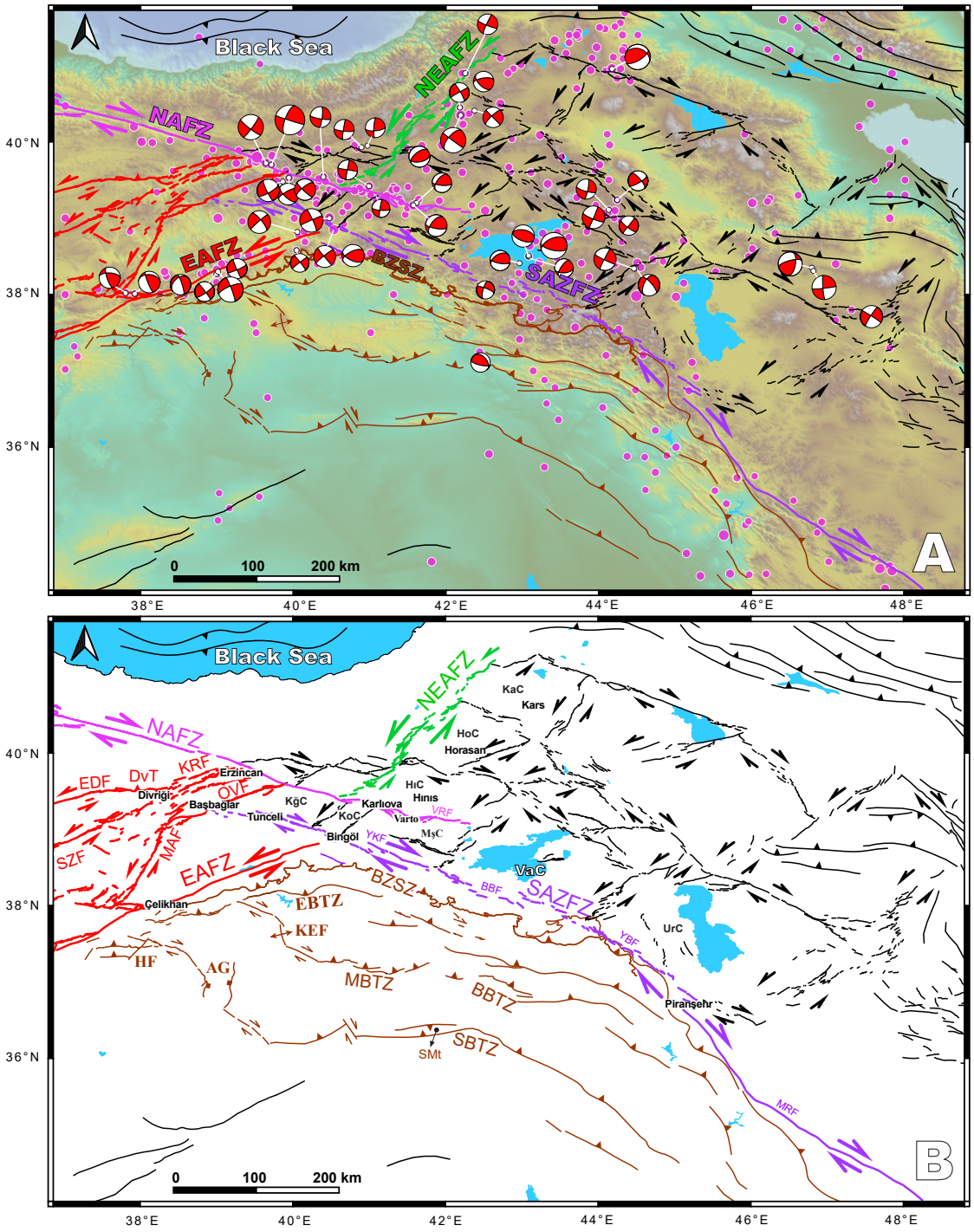

FIGURE 2. A) Main shear zones and the focal mechanism solutions of the seismic events in Turkish-Iranian Plateau and southeastern Turkey, northern Syria, and Iraq. Fault lines from Barrier *et al.* (2004); Emre *et al.* (2013) and Seyitoğlu *et al.* (2017a, 2018, 2022a). Focal mechanism solutions from Tan *et al.* (2008) and Global CMT Catalogue from Ekström *et al.* (2012). Pink dots with white circles represent the earthquake epicenters of magnitude ≥5 obtained from the Kandilli Observatory and Earthquake Research Institute (KOERI) catalogue. NAFZ: North Anatolian Fault Zone; SAZFZ: Southeast Anatolian Zagros Fault Zone; EAFZ: East Anatolian Fault Zone; NEAFZ: Northeast Anatolian Fault Zone; BZSZ: Bitlis-Zagros Suture Zone. B) Details of the structures in the same area. KRF: Karaca Fault; EDF: Ecemiş-Deliler Fault; DvT: Divriği Thrust; OVF: Ovacık Fault; SZF: Sarız Fault; MAF: Malatya Fault. Brown lines are Southeast Anatolian Wedge structures. SBTZ: Sincar-Kerkük Blind Thrust Zone; BBTZ: Bikhayr Blind Thrust Zone; EBTZ: Ergani-Silvan Blind Thrust Zone; MBTZ: Mardin Blind Thrust Zone; HF: Halfeti Fault; KEF: Karacadağ Extensional Fissure; AG: Akçakale-Harran Graben; SMt: Sincar Mountain. The rhomboidal cells whose margins define the main shear zones. KğC: Kiğı cell; KoC: Karlıova cell; MşC: Muş cell; VaC: Van cell; UrC: Urmiye cell; HıC: Hınıs cell; HoC: Horasan cell; KaC: Kars cell; VRF: Varto Fault; YKF: Yenisu-Kavakbaşı Fault; BBF: Bitlis-Bahçesaray Fault; Yüksekova_Bukan Fault; MRF: Main Recent Fault.

RESULTS

Southeast Anatolia

Southeast Anatolia is evaluated together with eastern Anatolia as East Anatolian Contractional Province by Şengör *et al.* (1985). In their neotectonic map, E-W trending fold axes and thrust faults with N-S trending Akçakale graben and Karacadağ extensional fissure were the main neotectonic elements in southeast Anatolia (Fig. 1A). On the other hand, dominant strike-slip faults and blind thrusts are presented in the regional map of Perinçek *et al.* (1987). The work of Biddle *et al.* (1987) was a good example of how the structures in southeast Anatolia should be examined in terms of folding and faulting relationship.

The Southeast Anatolian Wedge (SEAW) in cross sectional view is bounded by the Bitlis-Zagros Suture Zone in the north and the Sincar (Sinjar) Mountain in the south (Seyitoğlu *et al.*, 2017a) (Fig. 2A, B). Its internal structure is composed of south vergent thrusts and blind thrusts that are recognized mainly by using the positions of the asymmetrical anticlines at the hanging wall of the thrust faults. In map view, different southward moving thrust sheets are separated by tear faults. The NW-SE trending tear faults are generally right-lateral strike-slip in nature and the Karacadağ extensional fissure and Akçakale-Harran graben are developed in their releasing offset areas (Seyitoğlu *et al.*, 2017a). The NE-SW trending tear faults have left-lateral strike-slip kinematics and the Halfeti Fault is a well-examined example that is developed parallel to the East Anatolian Fault Zone (EAFZ) (Şahbaz and Seyitoğlu, 2018) (Fig. 2A, B).

The majority of seismic activity is related to these tear faults, but thrust-related earthquakes, although they are rare, give a clue about the internal structure of SEAW. One of the well-known examples of thrust-related seismic events is the 1975.09.06 (M=6.7) Lice earthquake (Arpat, 1977; Jackson and McKenzie, 1984). This earthquake was generally misinterpreted as evidence for activity of the Bitlis-Zagros Suture Zone (Emre *et al.*, 2013) probably due to reported surface deformations near the suture zone (Arpat, 1977). The epicentral location and depth of the hypocenter indicate that the 1975.09.06 (M=6.7) Lice earthquake is related to the Ergani-Silvan Blind Thrust Zone (Seyitoğlu *et al.*, 2017a). The other example of thrust-related earthquakes in the Southeast Anatolian Province is the 2012.06.14 (Mw=5.1) Cizre-Silopi earthquake. The epicenter location and depth of hypocenter show that this earthquake is related to the Bikhayr Blind Thrust Zone (Seyitoğlu *et al.*, 2017a) (Fig. 2). As seen in the two above examples of thrust-related earthquakes, the blind thrusts are capable of generating major earthquakes in the SEAW. When we consider the other mapped thrust and blind thrusts together with the tear faults, it can be said that southeast Anatolia is characterized by a considerable seismic hazard.

East Anatolia

Eastern Anatolia is considered a key location to study continental deformation caused by collision along the Bitlis-Zagros Suture Zone. Contractional tectonic activity initiated in the Late Maastrichtian-Early Eocene and is continuing today (Aktaş and Robertson, 1984; Aktuğ *et al.*, 2016; Allen, 2010; Hall, 1976; Reilinger *et al.*, 2006; Şengör and Kidd, 1979; Şengör and Yılmaz, 1981; Yılmaz, 1993). The collision between Arabian and Eurasian plates was suggested to be accommodated by thick continental crust (Dewey *et al.*, 1986). Later studies, however, proposed that East Anatolia is composed of an accretionary complex supported by asthenosphere (Şengör *et al.*, 2003, 2008). There are other studies proposing the existence of the continental basement under the Neogene cover (Topuz *et al.*, 2017). The fundamental neotectonic structures composed of left- and right-lateral strike-slip faults, E-W trending thrusts, and N-S normal faults developed under the N-S contraction in East Anatolia have been determined by Şengör *et al.* (1985).

The Turkish-Iranian Plateau including eastern Anatolia is located towards the hinterland of Bitlis-Zagros Suture Zone. The results of the ongoing continental collision, the associated active faults, and the related seismicity have been explained by the rhomboidal cell model (Seyitoğlu *et al.*, 2018) (Fig. 2A, B). Rhomboidal cells are limited by the NW-SE trending right- and NE-SW trending left-lateral strike-slip faults. Commonly, E-W thrusts and/or N-S normal faults are developed in the center of the cell. In other cases, the right- and left-lateral strike-slip boundary faults are connected by thrust faults at the northern and/or southern corners of the cell (Seyitoğlu *et al.*, 2018).

In the Turkish-Iranian Plateau several rhomboidal cells have been determined. It can be seen in the map that some of the margins of the cells align in one direction, and they can help to determine the region-wide shear zones (Fig. 2A, B). For example, Northeast Anatolian Fault Zone (NEAFZ) is composed of the NE-SW trending left-lateral strike-slip faults bounding the NW margins of the Kars, Horasan, and Hınıs rhomboidal cells. Moreover, NE margins of Kiğı, Karlıova, and Muş rhomboidal cells represent the easternmost continuation of the North Anatolian Fault Zone (NAFZ) (Seyitoğlu *et al.*, 2018) (Fig. 2B). Especially, the NE margin of Muş cell, the Varto Fault demonstrates that NAFZ does not terminate in the Karlıova as generally accepted in the tectonic escape model (Şengör *et al.*, 1985). The position of cells also provides a solution to the long-lasting problem of the relationship between NAFZ and the Main Recent Fault of Iran (Jackson, 1992). The southwest

margin of Kığı, Muş, Van, and Urmiye cells constitutes the Southeast Anatolian-Zagros Fault Zone (SAZFZ) including the Main Recent Fault. The newly defined Bitlis-Bahçesaray Fault showing recent high seismicity is a key element to connect the structures of Yenisu-Kavakbaşı Fault and Yüksekova-Bukan Fault in the SAZFZ (Seyitoğlu *et al.*, 2018, 2020) (Fig. 2B).

The focal mechanism solutions demonstrate that margins of the cells mainly produce strike-slip events and thrust related earthquakes occur in the north and south corners of the cells (*i.e.* 2001.07.10, Mw=5.6 at Hınıs cell; 2020.06.21, Mw=4.1 at Ağrı cell) or in the center of the cell (*i.e.* 2011.10.23, Mw=7.1 at Van cell) (Fig. 2A, B).

It is interesting to note that Lice and Van earthquakes are related to blind thrust faults in the Southeast and East Anatolian provinces, but they occurred in different tectonic settings. While the 1975.09.06 (M=6.7) Lice earthquake is related to a thrust within the SEAW in the foreland of BZSZ, the 2011.10.23 (Mw=7.1) Van earthquake is associated with a thrust in the center of rhomboidal cell in the hinterland of BZSZ (Fig. 2A).

The overall neotectonic framework in the East Anatolian Province shows that the NAFZ creates a releasing stepover with the SAZFZ where the Kığı, Karlıova, and Muş rhomboidal cells are developed (Seyitoğlu *et al.*, 2018). SAZFZ cut and displaces the EAFZ around Bingöl (Fig. 2A; B). The relationship between NAFZ and NE-SW

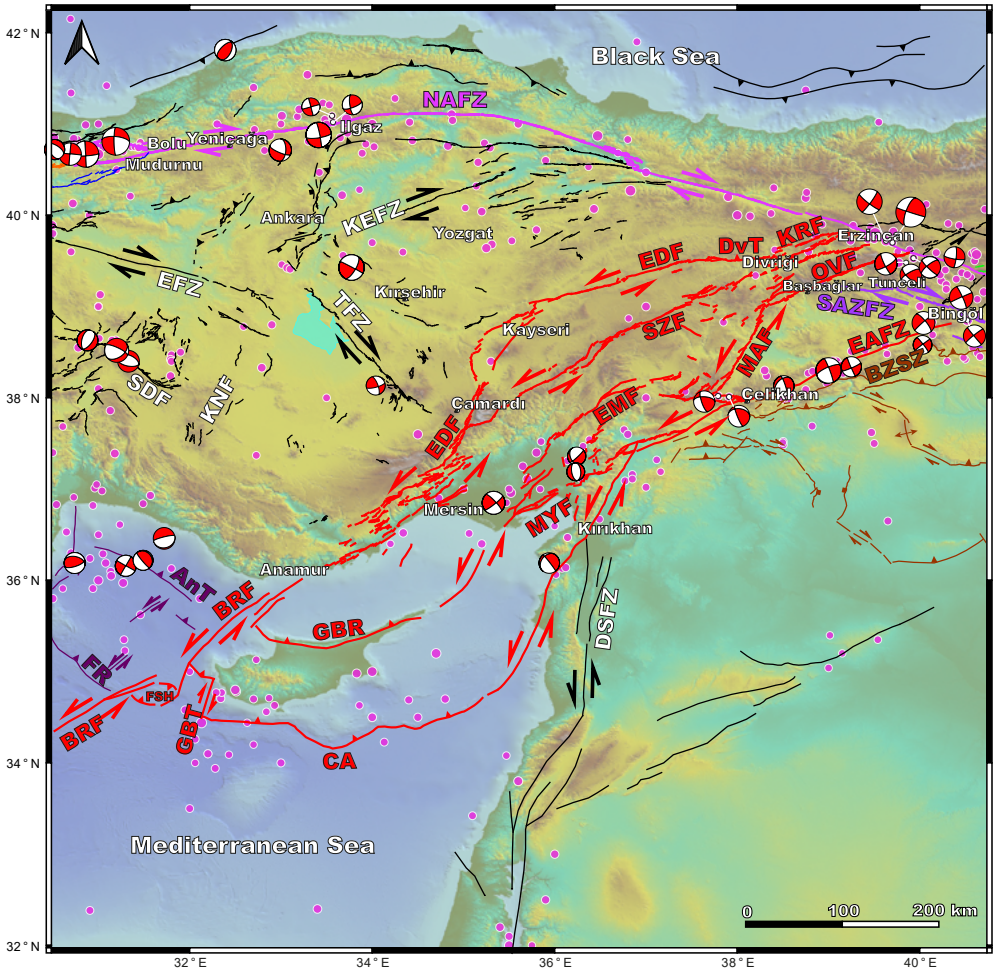

FIGURE 3. The active faults and the focal mechanism solutions of major seismic events between eastern and central Anatolia. Fault lines from Barrier *et al.* (2004); Emre *et al.* (2013); Seyitoğlu *et al.* (2022a). Focal mechanism solutions from Tan *et al.* (2008), Esat *et al.* (2020), and Global CMT Catalogue (Ekström *et al.*, 2012). Pink dots with white circles represent the earthquake epicenters of magnitude ≥5 obtained from the KOERI catalogue. NAFZ: North Anatolian Fault Zone; SAZFZ: Southeast Anatolian Zagros Fault Zone; EAFZ: East Anatolian Fault Zone; DSFZ: Dead Sea Fault Zone; BZSZ: Bitlis-Zagros Suture Zone; KEFZ: Kırıkkale-Erbaa Fault Zone; TFZ: Tuzgölü Fault Zone; EFZ: Eskişehir Fault Zone; SDF: Sultandağı Fault; KNF: Konya Fault. The Anatolian Diagonal Shear Zone, KRF: Karaca Fault; EDF: Ecemiş-Deliler Fault; DvT: Divriği Thrust; OVF: Ovacık Fault; SZF: Sarız Fault; MAF: Malatya Fault; EMF: Elbistan-Misis Fault; MYF: Maraş-Yumurtalık Fault; BRF: Biruni Fault; FSH: Fuat Sezgin High; GBT: Gazi Baf Transform; GBR: Girne-Beşparmak Range; CA: Cyprus Arc. The accompanying structures of the Anatolian Shear Zone, AnT: Antalya Thrust; FR: Florence Rise.

trending left-lateral structures parallel to the EAFZ will be discussed in the following section.

Transition between East and Central Anatolia

The neotectonic meaning of Anatolian Diagonal is defined in a paper (Seyitoğlu *et al.*, 2022a) which separates mainly the East Anatolian Province from the Central Anatolia (Fig. 3). The Anatolian diagonal is a left-lateral shear zone between the EAFZ (Şaroğlu *et al.*, 1992b; Herece, 2008; Duman and Emre, 2013) and the Central Anatolian Fault Zone (CAFZ) (Koçyiğit and Beyhan, 1998), referred to as Karaca, Ecemiş-Deliler, and Biruni faults, with a 170km width (Fig. 3). Its length reaches 850km between Erzincan and Cyprus. The internal deformation of the Anatolian Diagonal may be reflected in palaeomagnetic data (Tatar *et al.*, 2000) and internal structures such as the Sarız, Malatya, Ovacık, Elbistan-Misis and Maraş-Yumurtalık faults may play an important role (Fig. 3).

There are two important findings related to the Anatolian Diagonal concept. The first one is to bring new explanations for the relationship between right- and left-lateral major strike-slip faults. The classical tectonic escape model of Şengör *et al.* (1985) accepts a single intersection point in Karlıova between right-lateral NAFZ and left-lateral EAFZ. However, the Anatolian Diagonal concept together with the rhomboidal cell model for

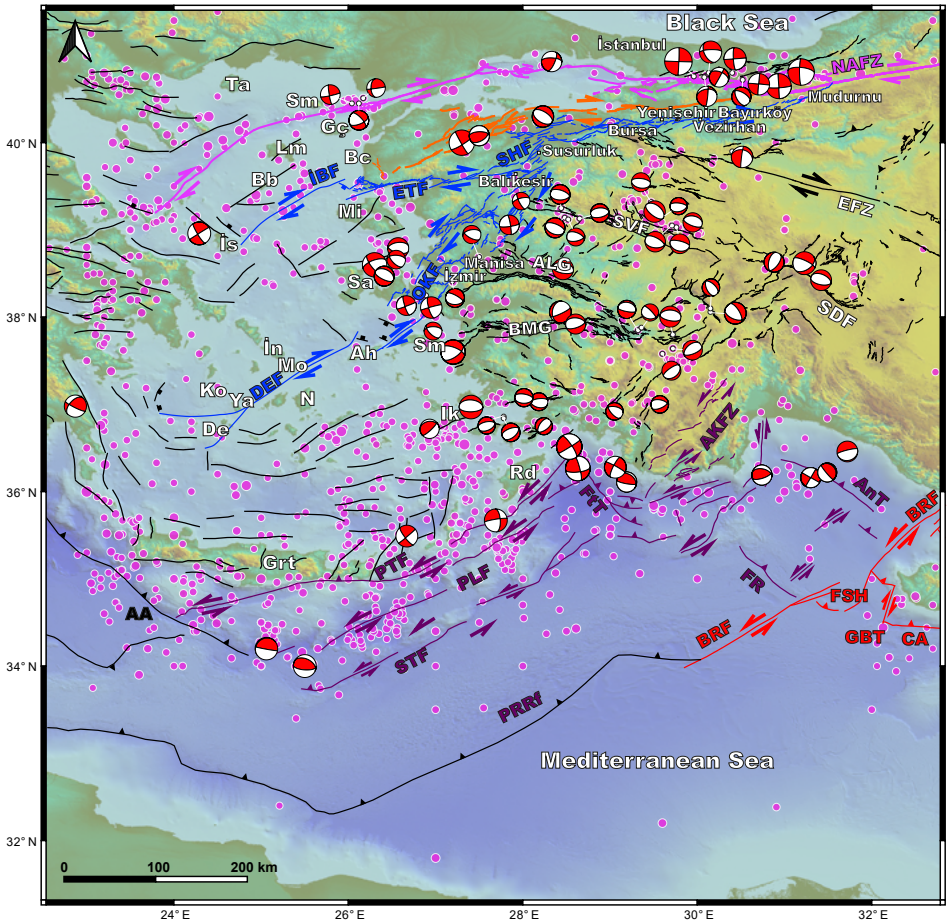

FIGURE 4. The active faults and the focal mechanism solutions of major seismic events in western Türkiye, the Aegean Sea, and Greece. Fault lines from Barrier *et al.* (2004); Caputo and Pavlides (2013); Emre *et al.* (2013); Seyitoğlu *et al.* (2022a, b). Focal mechanism solutions from Tan *et al.* (2008), Global Centroid Moment Tensor (CMT) Catalogue (Ekström *et al.*, 2012), Seyitoğlu *et al.* (2015a, 2022b). Pink circles represent the earthquake epicenters of magnitude ≥5 obtained from the Kandilli Observatory and Earthquake Research Institute (KOERI) catalogue. NAFZ: North Anatolian Fault Zone (northern branch: fuchsia lines; middle branch: orange lines; southern branch: blue lines). İBF: İskiri_Biga Fault; ETF: Edremit Fault; SHF: Susurluk-Havran Fault; OKF: Orhanlı-Karabağ Fault; DEF: Değirmenlik Fault. EFZ: Eskişehir Fault Zone; SVF: Simav Fault; SDF: Sultandağı Fault; ALG: Alaşehir Graben; BMG: Büyük Menderes Graben. The Anatolian Diagonal Shear Zone (red lines), BRF: Biruni Fault; FSH: Fuat Sezgin High; GBT: Gazi Baf Transform; CA: Cyprus Arc. Accompanying structures of the Anatolian Shear Zone, AnT: Antalya Thrust; FR: Florence Rise; AKFZ: Antalya-Kekova Fault Zone; FtT: Fethiye Thrust; PTF: Ptolemy Fault; PLF: Pliny Fault; STF: Strabo Fault. AA: Aegean Arc; PRRf: Piri Reis Ridge front. Aegean Islands: Grt: Girit (Crete); Rd: Rodos (Rhodes); De: Değirmenlik (Milos); Ya: Yavuzca (Syros); Mo: Mokene (Mikonos); İn: İstendin (Tinos); Ko: Koyunluca (Serifos); İk: İstanköy (Kos); Ah: Ahikerya (Ikeria); N: Nakşa (Naxos); Sm: Sisam (Samos); Sa: Sakız (Chios); Mi: Midilli (Lesvos); İs: İskiri (Skyros); Bb: Bozbaba (Agios Efstratios); Lm: Limni (Limnos); Bc: Bozcaada; Gç: Gökçeada; Sm: Semadirek (Samothraki); Ta: Taşoz (Thasos).

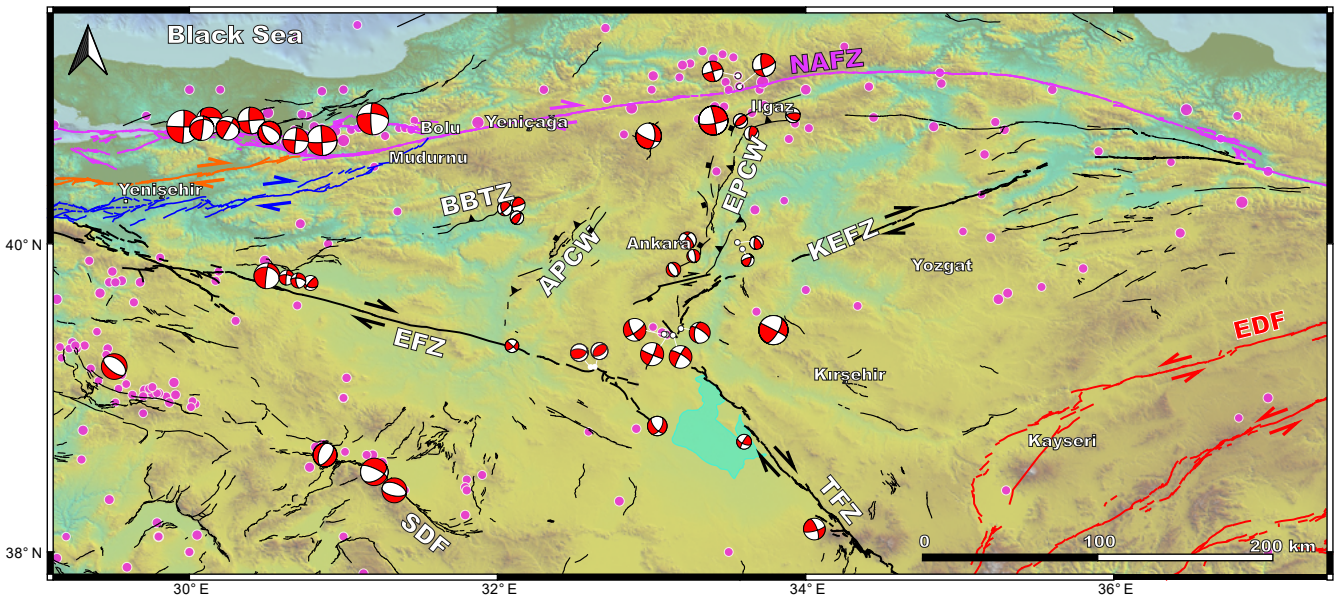

FIGURE 5. The active faults and the focal mechanism solutions of major seismic events in NW central Anatolia. Fault lines from Seyitoğlu *et al.* (2009, 2015a, 2016, 2017); Emre *et al.* (2013); Esat *et al.* (2014, 2016, 2017). Focal mechanism solutions (magnitude ≥3) from Tan *et al.* (2008), Global CMT Catalogue (Ekström *et al.*, 2012), Seyitoğlu *et al.* (2009, 2015a, b, 2017b), Esat *et al.* (2014, 2016, 2021). Pink dots with white circles represent the earthquake epicenters of magnitude ≥5 obtained from the KOERI catalogue. NAFZ: North Anatolian Fault Zone (northern branch: fuchsia lines; middle branch: orange lines; southern branch: blue lines); EFZ: Eskişehir Fault Zone; KEFZ: Kırıkkale-Erbaa Fault Zone; EPCW: Eldivan-Elmadağ Pinched Crustal Wedge; APCW: Abdüsselam Pinched Crustal Wedge; BBTZ: Beypazarı Blind Thrust Zone; TFZ: Tuz Gölü Fault Zone; SDF: Sultandağı Fault; EDF: Ecemiş-Deliler Fault and other faults belong to the Anatolian Shear zone (red lines).

eastern Turkey (Seyitoğlu *et al.*, 2018) demonstrate that multiple intersection points exist, and this creates a more complex relationship between right- and left-lateral strike-slip faults (Figs. 2B; 3). The left-lateral strike-slip Karaca Fault (KRF) belonging to the Anatolian Diagonal meets with the NAFZ west of Erzincan. This fault is connected to the Ecemiş-Deliler Fault (EDF) with a restraining bend where the Divriği Thrust (DvT) is developed. Southeast of Erzincan, the Ovacık Fault (OVF) is connected to the NAFZ and continues to the southwest limiting the SAZFZ around Başbağlar. Following an angular segment boundary, it is connected to the SSW with the Malatya Fault (MAF) (Fig. 3). In the Bingöl area, however, the SAZFZ cuts the EAFZ of the Anatolian Diagonal where the highest strain accumulation occurred (Seyitoğlu *et al.*, 2018). As summarized above at least four intersection points between right-lateral and left-lateral strike-slip faults show that the single intersection suggestion of the tectonic escape model (Şengör *et al.*, 1985) is too simplified (Seyitoğlu *et al.*, 2022a).

As a second important contribution of the Anatolian Diagonal concept, it helps to explain the relationship between Cyprus and Aegean arcs. The offshore continuation of the left-lateral strike-slip EDF, the Biruni Fault (BRF) is determined by the re-evaluation of seismic reflection lines of Mansfield (2005). We interpreted that this fault line continues further southwest connecting to the Piri Reis (eastern Mediterranean) Ridge Front by passing the Cyprus Arc (Figs. 3; 4) (Seyitoğlu *et al.*, 2022a).

The en echelon, right stepping left-lateral strike-slip Antalya-Kekova Fault Zone, one of the accompanying structures to the Anatolian Diagonal, creates a restraining stepover in which Florence Rise and thrusts in the Antalya basin are developed (Seyitoğlu *et al.*, 2022a). There is another restraining stepover where the thrust-related northern margin of the Rhodes basin developed between Antalya-Kekova Fault Zone and Pliny/Strabo faults (Fig. 4). In this fault configuration, the Antalya-Kekova Fault Zone is an alternative for the highly debated Burdur-Fethiye Fault Zone (see below). The southwest motion of the Anatolian plate indicated by the GNSS data can be realized mainly by the NAFZ and the Anatolian Diagonal Shear Zone and associated structures such as the Antalya-Kekova Fault Zone and Pliny-Strabo Fault (Seyitoğlu *et al.*, 2022a) (Fig. 4).

Central Anatolia

A triangular block of the Kırşehir-Yozgat area limited by the left-lateral EDF and right-lateral Kırıkkale-Erbaa Fault (Seyitoğlu *et al.*, 2009; Şengör *et al.*, 1985) moves towards WSW (Figs. 3; 5). The Tuzgölü Fault constitutes

the NW-SE trending margin of this triangular area. The Tuzgölü Fault is first evaluated as a right-lateral strike-slip fault with thrust component (Şaroğlu *et al.*, 1987). This structure together with the thrust related Sultandağ Fault (Boray *et al.*, 1985; Şaroğlu *et al.*, 1987) were used as evidence of NE-SW contraction in the Central Anatolian "Ova" province (Şengör *et al.*, 1985) (Fig. 1A). On the other hand, normal fault-related earthquakes of the 2000.12.15 (Mw=6.0) Sultandağ (Taymaz and Tan, 2001) and the 03.02.2002 (Mw=6.5) Çay (Başokur *et al.*, 2002; Emre *et al.*, 2003) changed the earlier neotectonic perception of Central Anatolia (Fig. 3).

The recent studies (Krystopowicz *et al.*, 2020; Kürçer and Gökten, 2014; Özsayın *et al.*, 2013) re-define the Tuzgölü Fault as a normal fault and/or normal fault with a right-lateral strike-slip component, but recent seismic activity at three different locations at Bala, Şereflikoçhisar, and Obruk indicate that the Tuzgölü Fault behaves as a right-lateral strike-slip fault as documented by the focal mechanism solutions (Esat *et al.*, 2014, 2020) (Fig. 5).

Although the current Sultandağ Fault is accepted as a normal fault, its earlier reverse fault behaviour was claimed in the southwest margin of Afyon-Akşehir graben (Koçyiğit *et al.*, 2000). However, Kaya *et al.* (2014) performed seismic reflection studies in this location and demonstrate no reverse fault history supporting the two-stages graben model (Fig. 5).

In northwest Central Anatolia, the area between the NAFZ, Kırıkkale-Erbaa Fault Zone (KEFZ) (Şengör *et al.*, 1985) and Eskişehir Fault Zone (EFZ) (Esat *et al.*, 2016; Seyitoğlu *et al.*, 2015a) is under influence of northwest-southeast contraction (Esat *et al.*, 2021; Seyitoğlu *et al.*, 2000) creating the Eldivan-Elmadağ Pinched Crustal Wedge (EPCW) (Seyitoğlu *et al.*, 2009), the Abdüsselam Pinched Crustal Wedge (APCW) (Esat *et al.*, 2017) and the Beypazarı Blind Thrust Zone (BBTZ) (Ardahanlıoğlu *et al.*, 2020; Seyitoğlu *et al.*, 2017b) with considerable seismic activity (Fig. 5).

The EPCW and APCW are both, NNE-SSW trending structures having thrusts and normal faults at their eastern and western margins respectively (Esat *et al.*, 2017; Seyitoğlu *et al.*, 2009). A local seismic network AnkNET was operational between 2007-2010 and its data were used to obtain focal mechanism solutions of the earthquakes around Ankara. The results support our field observations that the western normal faulted and eastern thrust faulted margins of the EPCW are active, and they are capable to produce earthquakes including the 2000.06.06 (Mw=6.0) Orta (Taymaz *et al.*, 2007) and the 2015.05.12 (M=4.0) Elmadağ earthquakes. Although different evaluations exist about the geology of the Ankara-Ayaş-Orta-Çankırı area (*i.e.* Adıyaman *et al.*, 2001; Kaymakçı *et al.*, 2001; Koçyiğit *et al.*, 2001; Rojay and Karaca, 2008; Seyitoğlu *et al.*, 2004b), it can be said by combining the InSAR evaluations of Çakır and Akoğlu (2008) and the focal mechanism solutions that the 2000.06.06 (Mw=6.0) Orta earthquake and subsequent seismic events are related to the NW-SE trending, SW dipping normal fault surface corresponding to the western margin of the EPCW (Esat *et al.*, 2021; Seyitoğlu *et al.*, 2009).

The large-scale examples of thrust parallel - normal faulting, similar to the EPCW and APCW, can be seen in the Himalayas (Burchfiel and Royden, 1985; Fossen, 2000) and Makran accretionary wedge (Seyitoğlu *et al.*, 2019) and their development experimentally demonstrated (Chemenda *et al.*, 1995). The name "shortening-induced normal faults" is proposed by Ring and Glodny (2010) for structures similar to the western margin of EPCW (Seyitoğlu *et al.*, 2009).

The BBTZ (Ardahanlıoğlu *et al.*, 2020; Seyitoğlu *et al.*, 2017b) is another seismically active structure responsible for the minor earthquakes in the region (Fig. 5).

Apart from the contractional neotectonic province between the NAFZ, EFZ, and KEFZ, southwestern Anatolia plus Kırşehir massif move towards SW with counter-clockwise rotation (Çinku *et al.*, 2016) along with the left-lateral Anatolian Diagonal Shear Zone and recently defined right-lateral southern branch of NAFZ (Seyitoğlu *et al.*, 2016, 2022b) between Bolu and Değirmenlik (Milos) island.

Western Anatolia

A north-south line of transition between central and western Anatolia was proposed around Afyon (Şengör *et al.*, 1985) (Fig. 1A). Later, Barka and Reilinger (1997) proposed a recumbent V-shaped border between western and central Anatolia which is drawn by the Eskişehir Fault Zone (EFZ) and Fethiye-Burdur Fault Zone (FBFZ) (Fig. 1B). As mentioned in the Central Anatolia section, normal fault-related earthquakes (Sultandağ 2000.12.15, Mw=6.0 and Çay 2002.02.03, Mw=6.5) suggested shifting the boundary between the western extensional province and central Anatolia in correspondence with the Tuzgölü Fault (Emre *et al.*, 2018; Koçyiğit and Özacar, 2003) (Fig. 1C, D).

The east-west trending structures in western Anatolia produce earthquakes whose focal mechanism solutions show pure normal faulting such as 1969.03.28 (Mw=6.4) Alaşehir; 1970.03.28 (Mw=7.0) Gediz; 2011.05.19 (Mw=5.8) Simav; 2017.07.21 (Mw=6.6) Bodrum and 2019.08.08 (Mw=6.0) Bozkurt (Fig. 4), even if some of

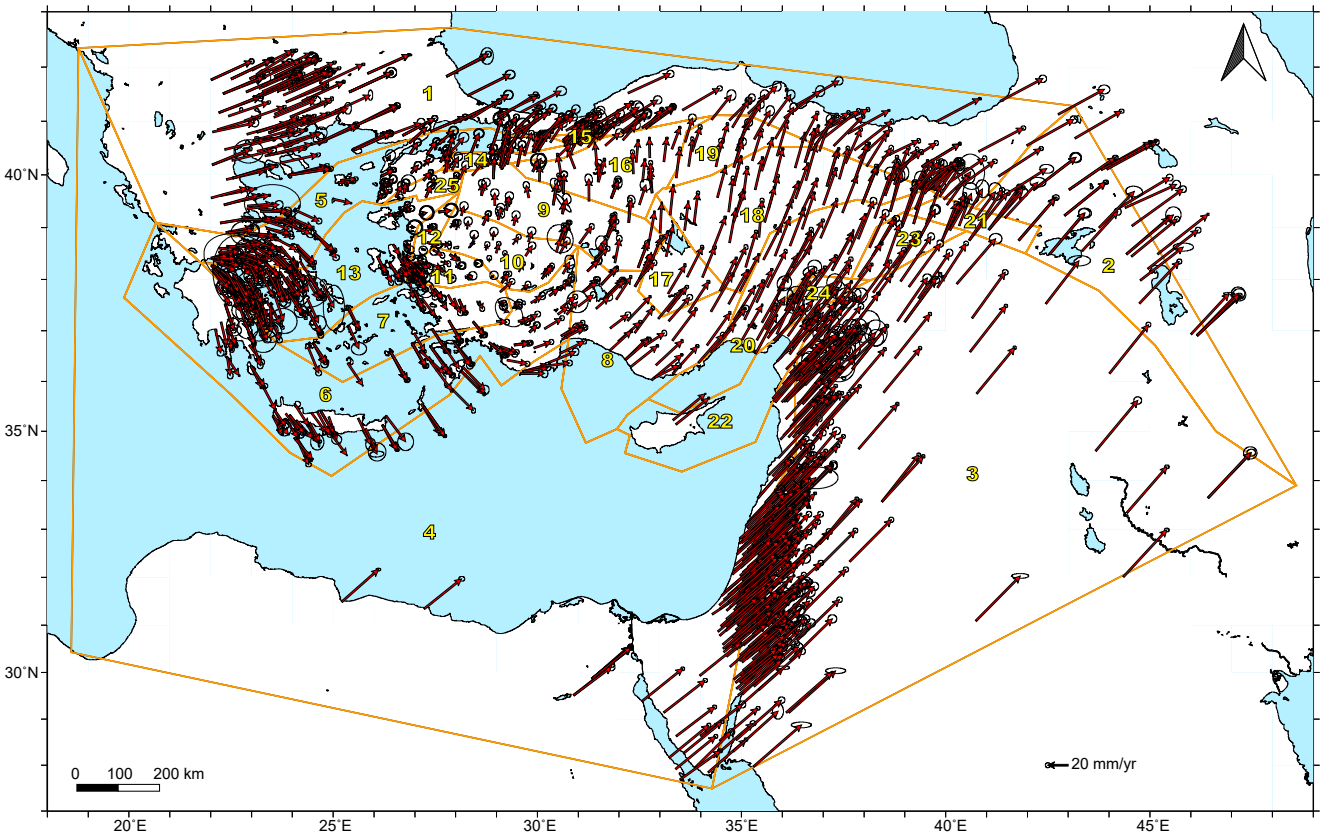

FIGURE 6. The discretization of the study domain and original GNSS velocities in ITRF08 given in (Kreemer *et al.*, 2014). Orange lines are block boundaries.

them (*i.e.* Simav Fault) shown as a right-lateral strike-slip structure in the active fault map of Turkey (Emre *et al.* 2013). The tectonic style and formation history of the east - west trending structures have been reviewed in Seyitoğlu and Işık (2015) and readers may refer to this paper having evolutionary 3D block diagrams.

The main problem in the NNE-SSW highly extending western Anatolia is to explain strike-slip-related earthquakes. While some scientists attribute to these structures a left- (Ring *et al.*, 1999) or right-lateral transfer zone (Uzel *et al.*, 2013; Uzel and Sözbilir, 2008), others suggest a "bend model" (Emre *et al.*, 2018) in northwestern Anatolia which however does not explain the strike-slip related seismic events further south around İzmir (Fig. 4).

Crampin and Evans (1986) proposed that the southern branch of NAFZ may extend to İzmir. Other studies also show this branch in their general fault maps (Ocakoğlu *et al.*, 2005; Yaltırak *et al.*, 2012). Seyitoğlu *et al.* (2022b) provide segment distribution of the southern branch of NAFZ extended between Bolu to Değirmenlik (Milos) island via Gölpazarı, Bursa, Balıkesir, Manisa and İzmir (Fig. 4).

We know that extensional tectonics was established in the region since the Oligocene times (Seyitoğlu *et al.*, 2004a), and this is earlier than the triggering event of the tectonic escape model (Seyitoğlu and Scott, 1996b). The strike-slip faults may operate as transfer faults between the major normal faults under the extensional tectonic regime (*i.e.* Şengör, 1987) and they should be retained between normal faults as the nature of transfer faults. However, the distribution of strike-slip-related earthquakes can be seen from Susurluk valley to the south of İzmir beyond the major normal faults (Fig. 4). This observation supported the existence of a shear zone attributed to the southern branch of NAFZ in western Turkey in which its X-fractures are capable to produce moderate earthquakes such as recent the 2020.01.22 (Mw=5.5) Musalar-Akhisar earthquake. Moreover, the focal mechanism solutions of the 2020.10.30 (Mww=7.0) Sisam (Samos) earthquake's aftershocks clearly demonstrate that Ahikerya (Ikaria) depression can be evaluated as a pull-apart structure that is developed along the southern branch of NAFZ (Seyitoğlu *et al.*, 2022b).

The existence of left-lateral FBFZ is another highly debated scientific problem in the region. Some researchers suggest that northeast continuation of Pliny/Strabo Faults

can be followed in southwest Anatolia (Elitez *et al.*, 2016; Hall *et al.*, 2014; ten Veen *et al.*, 2009), but others mainly put forward an argument of the absence of any high magnitude left-lateral strike-slip seismic events and palaeomagnetic data (Howell *et al.*, 2017; Kaymakçı *et al.*, 2018). The solution to this problem may lie further southeast at the left-lateral strike-slip Antalya-Kekova Fault Zone which plays an important role between the Anatolian Diagonal and the Pliny/Strabo Faults by creating restraining stepovers on both sides (*i.e.* Antalya basin and northeastern of Rhodes basin) (Figs. 3; 4). The Antalya-Kekova Fault Zone and the Pliny/Strabo Faults, which are accompanying structures of the Anatolian Diagonal, may accommodate SW motion of the Anatolian Plate together with the NAFZ (Seyitoğlu *et al.*, 2022a).

Block modelling

The domain was discretized into 25 blocks (Fig. 6). Original GNSS velocities in ITRF08 given by Kreemer *et al.* (2014) are used for computing the block rotations (Fig. 6). The locking depth is taken constantly as 15km over the region and vertical faults are assumed. In this respect, estimated fault normal slips correspond to horizontal contraction rates. The velocities of 1498 GNSS sites which are located within the defined blocks were employed, which correspond to 2996 observations. The Euler rotations of 25 blocks are estimated, which correspond to 75 parameters. The overall fit of the observations has been computed by the WRMS which was found to be 2.1mm/yr. The velocity field given by Kreemer *et al.* (2014) is actually a compilation of the published velocities and they are homogeneous in terms of given precision. The formal uncertainties of the individual input velocities range from 0.1 to 4mm/yr. Considering the precision of the input velocities and the scale of the modeling 2.1mm/yr of WRMS seems consistent. The residual velocities are shown in Figure 7. The results also show that the proposed block model can model at least 90% of the slip rates considering the obtained WRMS of 2.1mm/yr and the average uncertainty of the input velocities which range from 0.1 to 4mm/yr. The overall reduced $\chi 2$ is 27.96 which is well below the theoretical table value of 3047.84 at a 95% confidence level. The individual statistics and goodness of fit values for each block are given in Table 1. The estimated relative Euler rotation vectors and the associated full covariance matrices for each pair of block rotations are given in Table 2.

TABLE 1. The statistics of block modelling for each block

Nº	Lon. (°)	Lat. (°)	#Site	wrms (mm)	χ^2	χ^2 (Table)
1	28.98606	41.16642	205	2.7	36.14	455.04
2	44.29859	38.19355	32	2.0	14.60	80.23
3	40.38142	33.80781	203	1.3	11.20	450.81
4	26.77626	32.66450	164	0.8	7.80	368.04
5	25.31671	39.55962	158	3.1	27.46	355.26
6	25.01418	36.45641	109	3.6	152.21	250.21
7	26.64564	37.11037	46	1.4	28.06	112.02
8	32.28707	36.72620	42	1.7	24.57	103.01
9	30.55094	39.19525	51	2.1	13.22	123.23
10	29.20414	38.55156	31	1.6	22.60	77.93
11	27.88212	38.17293	33	2.1	27.98	82.53
12	27.38659	38.89583	18	1.4	33.66	47.40
13	24.98840	38.16643	135	1.7	10.91	306.11
14	29.31841	40.32985	26	2.3	10.10	66.34
15	30.99440	40.68671	14	1.8	6.19	37.65
16	31.98593	40.13761	31	2.1	28.78	77.93
17	33.37392	38.20998	9	1.8	123.58	25.00
18	35.66547	39.46899	48	1.3	21.49	116.51
19	34.64416	40.54979	18	1.2	7.69	47.40
20	36.01707	37.79050	40	1.4	16.62	98.48
21	40.78687	39.08893	13	1.9	6.41	35.17
22	34.36014	35.38144	17	1.1	15.11	44.99
23	38.90614	38.66947	19	1.7	7.94	49.80
24	36.63119	37.55428	12	1.2	7.88	32.67
25	27.41379	39.77778	24	3.5	24.42	61.66

DISCUSSION

In southeast Anatolia, the southern border of SEAW, which is located south of Sincar Mountain (Seyitoğlu *et al.*, 2017a), is not taken into account as a block boundary because the reliability of the GNSS stations in northern Iraq and Syria is low due to ongoing war in the region. Therefore, the EAFZ and the SAZFZ are selected as block boundaries. The SAZFZ is composed of the southwestern borders of the Kiğı, Muş, Van and Urmiye rhomboidal cells at the hinterland of BZSZ and the Main Recent Fault of Zagros Mountains (Seyitoğlu *et al.*, 2018) (Fig. 2B). More detailed block determination is not allowed due to the lack of GNSS stations in the region (at least three GNSS stations are required to establish a block). We should note that the EAFZ and SAZFZ bear the strain on both SEAW in the foreland and the rhomboidal cells in the hinterland of BZSZ (Fig. 8A).

The overall results indicate consistent right-lateral slip rates ranging between -10.7±1.8 and -8.5±4.1mm/yr for the SAZFZ with only two exceptions. The first one is the southwest margin of the Muş rhomboidal cell, which has statistically insignificant results. The second exception is the segment at the southeast of Piranşehr (Iran) having higher extensional results (-9.2±0.9mm/yr) than the right-lateral slip rates (-7.4±1.2mm/yr) (Fig. 8A). This result is quite normal because the Piranşehr is the extensional stepover between the northwestern sector of the SAZFZ and that of the southeastern sector known previously as the "Main Recent Fault" (Figs. 2B; 8A).

The NAFZ extended from east of Varto to Greece is selected as a block boundary dominantly having right-lateral slip rate ranging between -9.8±3.1mm/yr and -25.6±1.1mm/yr with some exceptions in Almacık block

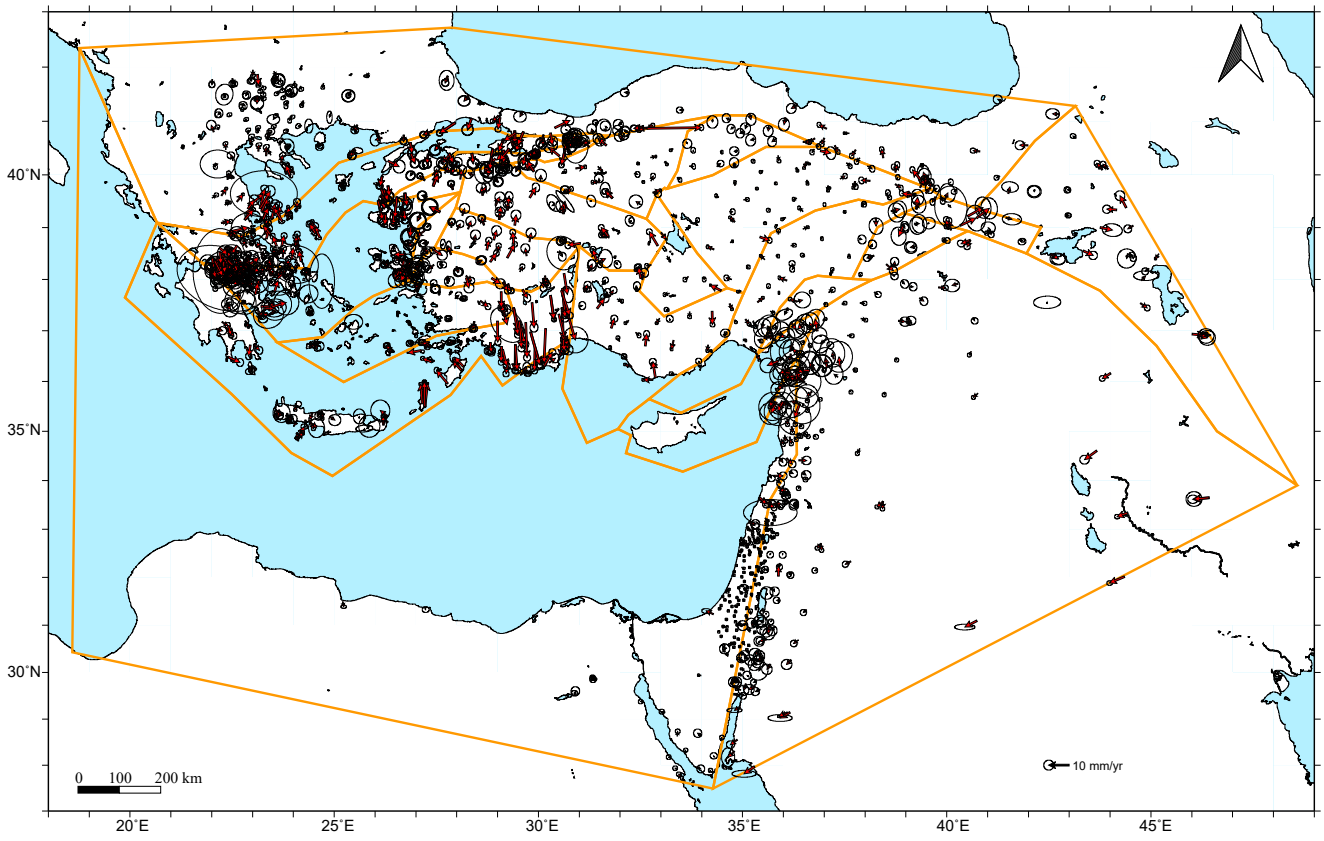

FIGURE 7. The residual velocity after removing rigid block motions and elastic strain along block boundaries.

and in Varto (-4.2±2.8mm/yr). The unexpectedly low slip rate in Varto relative to the rest of NAFZ probably results from the poor design of block boundary at the northwest margin of the Van cell where the cell boundary locations are uncertain due to the lack of detailed GNSS stations in the eastern Anatolia (see the real form of northwest margin of Van rhomboidal cell in Figure 2B). For this reason, the eastern edge of NAFZ terminated with a boundary that has no geological meaning and was marked with the yellow line. Please also note that probably due to this unrealistic but compulsory boundary, we have the segment providing statistically insignificant result at the southwest of the Muş cell that is connected to this yellow line (Figs. 2A, B; 8A).

One of the important block boundaries in eastern Turkey is the NEAFZ (Barka and Reilinger, 1997) which is represented by the northwest margins of Hınıs, Horasan, and Kars rhomboidal cells (Seyitoğlu *et al.*, 2018). The block boundary along this structure has left-lateral slip rates ranging between 3.4±0.8mm/yr and 3.2±0.8mm/yr (Figs. 2A, B; 8A).

The EAFZ, the southeast margin of the Anatolian Diagonal Shear Zone (Seyitoğlu *et al.*, 2022a), is cut by the SAZFZ and has significant left-lateral slip rates between Bingöl and Çelikhan ranging 19.2±2.8 and 14.8±2.6mm/yr. These slip rates dramatically decrease to 8.3±2.4 and 7.7±3.6mm/yr between Kırıkhan and Çelikhan where the Sürgü Fault separated from the EAFZ (Fig. 8A). The EAFZ is connected to the Cyprus Arc with Lazkiye (Latakhia) Fault which has a dominant extensional component (-7.6±1.3mm/yr) as well as left-lateral slip rates (4.9±1.2mm/yr) (Fig. 8B). To the south of Kırıkhan, the Dead Sea Fault reaches the Gulf of Aqaba with the left lateral slip rates ranging between 6.2±0.5mm/yr and 3.0±0.3mm/yr (Figs. 3; 8A, B).

The northwest margin of the Anatolian Diagonal Shear Zone is composed of Karaca Fault (KRF), Kemah-İliç Fault (KİF), DvT and EDF and its offshore continuation, the BRF (Seyitoğlu *et al.*, 2022a) (Figs. 3; 8B). This margin provides a connection between the NAFZ and the Cyprus Arc, for this reason, it is selected as a block boundary. The results are quite compatible with the tectonic style of the faults. The block boundary representing KRF and KİF has left-lateral and dominant contractional slip rates [1.8±1.6 (2.9±0.8)mm/yr]. The nearly E-W trending boundary signifying the Divriği Thrust has a dominant contractional

TABLE 2. The estimates of Euler rotations for each block pair and the associated covariance elements

BL1	BL2	Ωx (°/Myr)	Ωy (°/Myr)	Ωz (°/Myr)	$\sigma^2_{\Omega_X}$ (°/Myr)^2	$\sigma^2_{\Omega_Y}$ (°/Myr)^2	$\sigma^2_{\Omega_z}$ (°/Myr)^2	$\sigma_{\Omega_{XY}}$ (°/Myr)^2	$\sigma_{\Omega_{XZ}}$ (°/Myr)^2	$\sigma_{\Omega_{YZ}}$ (°/Myr)^2
2	1	-0.448521	-0.382709	-0.535808	0.011205	0.010564	0.013985	0.010800	0.012484	0.012098
21	1	-1.941241	-1.745933	-2.215660	0.760683	0.573137	0.876256	0.659811	0.815985	0.708108
20	1	0.412580	0.147716	0.226051	0.025333	0.013547	0.024031	0.018478	0.024631	0.018000
18	1	-0.302564	-0.439791	-0.500097	0.009573	0.004790	0.009808	0.006745	0.009671	0.006830
19	1	0.026658	-0.197024	-0.116588	0.283496	0.136572	0.307054	0.196660	0.294877	0.204660
16	1	-0.393990	-0.510080	-0.519657	0.074711	0.029020	0.073409	0.046524	0.074011	0.046114
15	1	4.920747	2.994948	4.770151	12.371438	4.382212	12.072092	7.361266	12.217520	7.271083
5	1	0.965295	0.284805	0.988031	0.007980	0.001648	0.006487	0.003603	0.007165	0.003247
4	1	-0.025503	-0.030044	-0.084136	0.001117	0.000425	0.000742	0.000674	0.000897	0.000535
3	2	0.650250	0.518739	0.587685	0.011539	0.010864	0.014099	0.011141	0.012695	0.012345
21	2	-1.492720	-1.363224	-1.679851	0.771174	0.583534	0.889584	0.670274	0.827791	0.719883
4	3	-0.227232	-0.166074	-0.136012	0.001451	0.000724	0.000856	0.001015	0.001108	0.000782
22	3	0.856996	0.512896	0.786364	0.069815	0.031602	0.050953	0.046914	0.059545	0.040047
24	3	-0.451570	-0.417891	-0.413903	0.745723	0.405110	0.679426	0.549454	0.711493	0.524461
23	3	1.401156	0.963224	1.413965	0.427249	0.282714	0.459153	0.347256	0.442446	0.359974
21	3	-2.142970	-1.881963	-2.267536	0.761017	0.573436	0.876371	0.660152	0.816195	0.708355
6	4	-0.231435	-0.272392	0.157438	0.003016	0.000833	0.001791	0.001553	0.002316	0.001190
8	4	-0.259741	-0.281240	-0.226795	0.024731	0.010169	0.019531	0.015837	0.021945	0.014066
22	4	1.084228	0.678970	0.922376	0.069884	0.031560	0.050924	0.046911	0.059554	0.040012
15	5	3.955452	2.710143	3.782120	12.378704	4.383693	12.077922	7.364532	12.224007	7.274006
14	5	0.403336	0.267238	0.266261	0.697217	0.228111	0.670801	0.398423	0.683489	0.390769
25	5	-3.689145	-1.931573	-3.905023	2.555891	0.681682	2.271468	1.319468	2.408763	1.243827
13	5	-0.135598	-0.088837	-0.076095	0.024891	0.004993	0.018507	0.011113	0.021413	0.009578
6	5	-1.222234	-0.587240	-0.914729	0.009879	0.002056	0.007535	0.004482	0.008584	0.003902
13	6	1.086636	0.498403	0.838634	0.019523	0.003921	0.013726	0.008727	0.016344	0.007309
7	6	0.937186	0.468459	0.708007	0.016369	0.003946	0.011119	0.008014	0.013458	0.006600
10	6	-0.262984	-0.220857	-0.656796	0.142503	0.043649	0.118322	0.078732	0.129692	0.071750
8	6	-0.028306	-0.008848	-0.384233	0.026226	0.010320	0.020495	0.016379	0.023144	0.014509
13	7	0.149449	0.029944	0.130627	0.031380	0.006883	0.022090	0.014646	0.026287	0.012276
11	7	-3.084740	-1.653617	-2.814508	0.488599	0.134291	0.383101	0.256048	0.432416	0.226674
9	8	0.513724	0.201097	0.391509	0.068717	0.026204	0.059697	0.042346	0.063919	0.039396
17	8	-0.241067	-0.228473	-0.310778	0.095727	0.041269	0.080832	0.062792	0.087889	0.057699
18	8	-0.017320	-0.128508	-0.189166	0.033186	0.014534	0.028597	0.021908	0.030718	0.020360
20	8	0.697824	0.458999	0.536982	0.048947	0.023291	0.042820	0.033641	0.045678	0.031531
22	8	1.343969	0.960210	1.149171	0.093095	0.041047	0.069628	0.061737	0.080383	0.053331
10	9	-0.748403	-0.413106	-0.664072	0.184993	0.059533	0.157524	0.104699	0.170467	0.096637
12	9	-1.964276	-0.975802	-1.586815	2.208081	0.600297	1.812856	1.150407	2.000103	1.042832
25	9	-2.952330	-1.536582	-2.997570	2.593015	0.696494	2.305890	1.343048	2.444469	1.266446
14	9	1.140151	0.662229	1.173714	0.734341	0.242923	0.705222	0.422003	0.719195	0.413388
16	9	-0.622471	-0.399894	-0.600234	0.119101	0.045312	0.113660	0.073369	0.116204	0.071656
17	9	-0.754791	-0.429570	-0.702287	0.116503	0.047817	0.102295	0.074474	0.109035	0.069711
11	10	-1.884569	-0.964300	-1.449704	0.614733	0.173994	0.490303	0.326766	0.548650	0.291824
12	10	-1.215873	-0.562695	-0.922743	2.303582	0.627077	1.889221	1.201078	2.085505	1.088061
12	11	0.668696	0.401605	0.526961	2.637821	0.714758	2.145635	1.372474	2.378286	1.238019
13	12	2.565493	1.281956	2.418173	2.180602	0.587350	1.784625	1.131072	1.972157	1.023621
25	13	-3.553547	-1.842736	-3.828928	2.565536	0.683547	2.277659	1.323713	2.416523	1.247234
15	14	3.552115	2.442905	3.515860	13.060676	4.608675	12.736406	7.756086	12.893844	7.658606
16	14	-1.762622	-1.062123	-1.773948	0.763948	0.255483	0.737723	0.441344	0.750335	0.433636
25	14	-4.092481	-2.198811	-4.171284	3.237863	0.906665	2.929953	1.711022	3.078600	1.628426
16	15	-5.314737	-3.505028	-5.289808	12.445435	4.411064	12.144844	7.407452	12.290852	7.316874
19	16	0.420649	0.313056	0.403069	0.357493	0.165424	0.379806	0.242846	0.368209	0.250451
18	16	0.091427	0.070289	0.019560	0.083570	0.033642	0.082560	0.052932	0.083003	0.052620
17	16	-0.132321	-0.029677	-0.102052	0.146110	0.060377	0.134795	0.093815	0.140174	0.089959
18	17	0.223747	0.099965	0.121613	0.080972	0.036148	0.071195	0.054037	0.075834	0.050675
19	18	0.329222	0.242767	0.383509	0.292355	0.141194	0.316206	0.203067	0.303869	0.211166
20	18	0.715144	0.587507	0.726148	0.034192	0.018169	0.033182	0.024886	0.033623	0.024507
21	20	-2.353821	-1.893649	-2.441711	0.785302	0.586516	0.899630	0.677952	0.839938	0.725785
23	20	1.190305	0.951538	1.239791	0.451534	0.295794	0.482413	0.365056	0.466188	0.377405
24	20	-0.662421	-0.429576	-0.588077	0.770008	0.418190	0.702686	0.567254	0.735236	0.541891
22	20	0.646145	0.501210	0.612189	0.094100	0.044682	0.074213	0.064714	0.083288	0.057477
23	21	3.544126	2.845187	3.681502	1.186883	0.855384	1.334639	1.006389	1.257543	1.067513
24	22	-1.308566	-0.930787	-1.200266	0.814156	0.435946	0.729494	0.595350	0.769940	0.563691
24	23	-1.852726	-1.381115	-1.827868	1.171589	0.687057	1.137694	0.895692	1.152841	0.883618

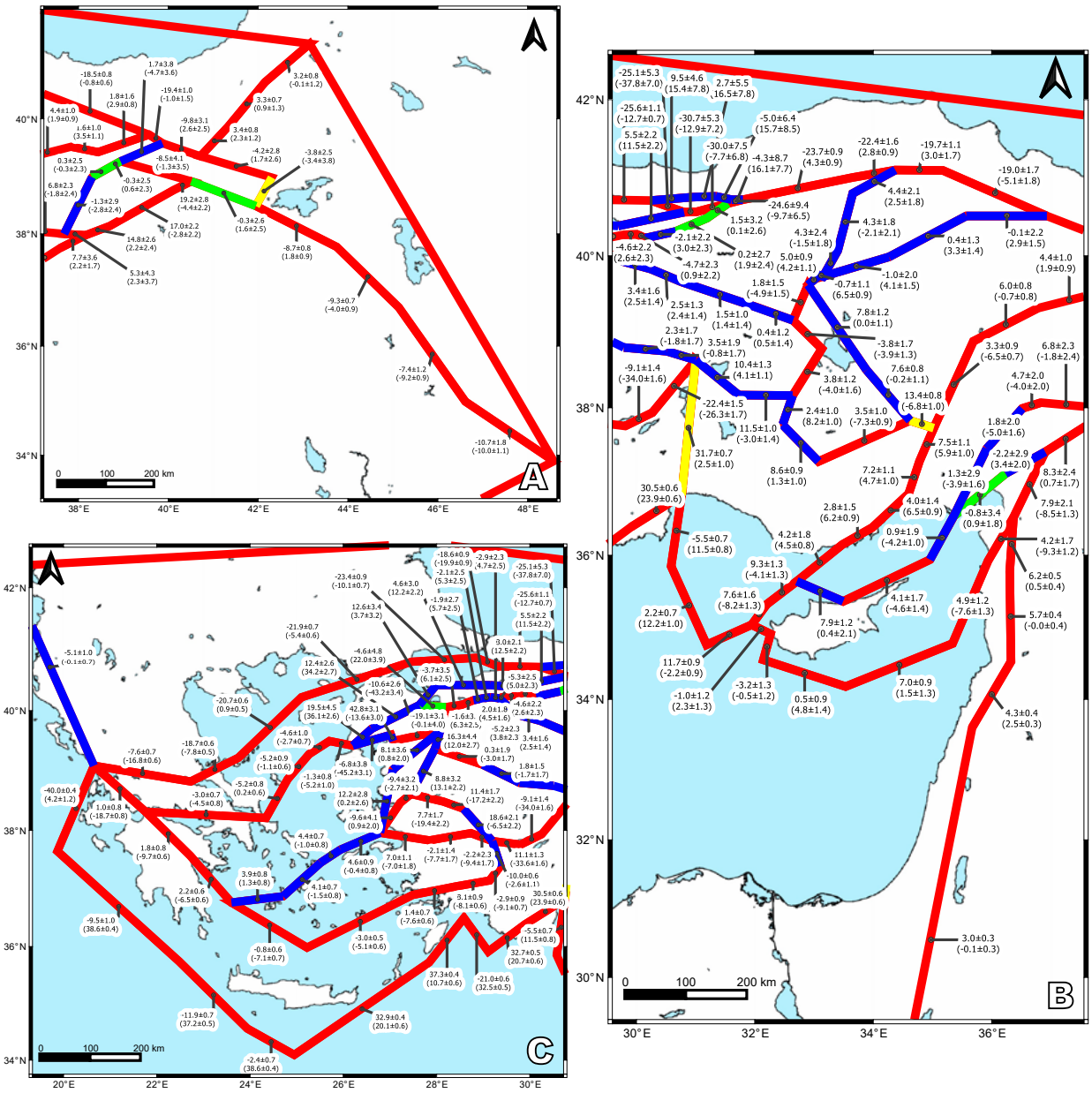

FIGURE 8. Inverted slip rates and 1-sigma uncertainties for main faults obtained in block modeling. The positive values correspond to left-lateral and reverse slips, respectively, for the fault-parallel and fault-normal (in parenthesis) slip rates. Based on the slip rates, red boundaries are both geologically and statistically meaningful; blue boundaries are statistically meaningful but not geologically; green boundaries are statistically meaningless. Yellow lines are not corresponding to a real tectonic border. A) Turkish-Iranian Plateau, eastern and southeastern Anatolia. B) Central Anatolia, Cyprus. C) Western Turkey, Aegean Sea, and Greece.

slip rate with left-lateral component [1.6±1.0 (3.5±1.1) mm/yr]. The block boundaries between Divriği and Kayseri have dominant left-lateral slip rates (*i.e.* 6.0±0.8mm/yr and 4.4±1.0mm/yr). The block boundary passing through Kayseri pull-apart basin (Dirik and Göncüoğlu, 1996; Koçyiğit and Beyhan, 1998) has a dominant extensional slip rate with left-lateral component [3.3±0.9 (-6.5±0.7) mm/yr] (Fig. 8B). The block boundaries between Çamardı and Mersin have nearly equal contractional and left-lateral slip rates [*i.e.* 7.5±1.1 (5.9±1.0)mm/yr and 7.2±1.1 (4.7±1.0)mm/yr]. Probably due to the orientation of the block boundary between Mersin and south of Anamur, the dominant slip is contractional with left lateral component (Figs. 3; 8B).

In the northwest and west of Cyprus, the block boundaries representing the offshore continuation of EDF, named as BRF, have considerable left-lateral slip rates [*i.e.*

11.7±0.9 (-2.2±0.9)mm/yr and 9.3±1.3 (-4.1±1.3)mm/yr] (Figs. 3; 8B).

It is interesting to see the contractional slip rates on the block boundary representing the Florence Rise (FR) [2.2±0.7 (12.2±1.0)mm/y], where different interpretations exist on its character in the literature. The slip rates obtained from block boundaries in southern and western Cyprus are concordant with the tectonic evaluation of Seyitoğlu *et al.* (2022a) which explains the relationship between the Anatolian Diagonal Shear Zone and Cyprus/Aegean arcs. In the west of Cyprus, the Gazibaf (Paphos) Transform Fault (GBT) presents right-lateral slip rate (-3.2±1.3mm/y) that connects the fragments of Cyprus Arc having contractional slip rates (*i.e.* 4.8±1.4mm/yr and 2.3±1.3mm/yr) (Figs. 3; 8B).

It is also important to note that the block boundaries representing the Antalya-Kekova Fault Zone (AKFZ), which are providing the connection of Cyprus and Aegean arcs, have important left-lateral slip rates (*i.e.* 30.5±0.6 and 32.7±0.5mm/yr). These values are similar to the slip rates obtained for the Pliny (PLF) and Strabo (STF) faults (37.3±0.4 and 32.9±0.4mm/yr) (Figs. 4; 8C). The block boundary at the northeastern Rhodes basin gives a contractional slip rate of 32.5±0.5mm/yr which is quite a concordant value for a place that is located on the contractional stepover between Antalya-Kekova Fault Zone and Pliny/Strabo Fault (Figs. 4; 8C).

The internal deformation of the Anatolian Diagonal Shear Zone, however, does not provide meaningful results probably because our generalized block boundaries are outlying to represent the details of the faults such as releasing or restraining stepovers (Fig. 8B).

We have the same problem for the block boundaries representing the internal deformation of central Anatolia. The block boundaries representing KEFZ, EFZ, Tuzgölü (TFZ) fault zones, Simav (SVF) (except one segment) and Konya (KNF) faults and EPCW have slip rates that are incompatible with their tectonic character determined by field observations (Fig. 8B). On the other hand, when the block modeling is performed at a smaller scale with more detailed block boundaries, the slip rate results are found compatible with their tectonic character in northwest central Anatolia. A recent block modelling study provides right-lateral slip rates for the EFZ (-5.4±2.9mm/yr) and KEFZ (-8.2±3.3mm/yr), TFZ (-5.0±2.3mm/yr) and more importantly 12.5±3.2mm/yr

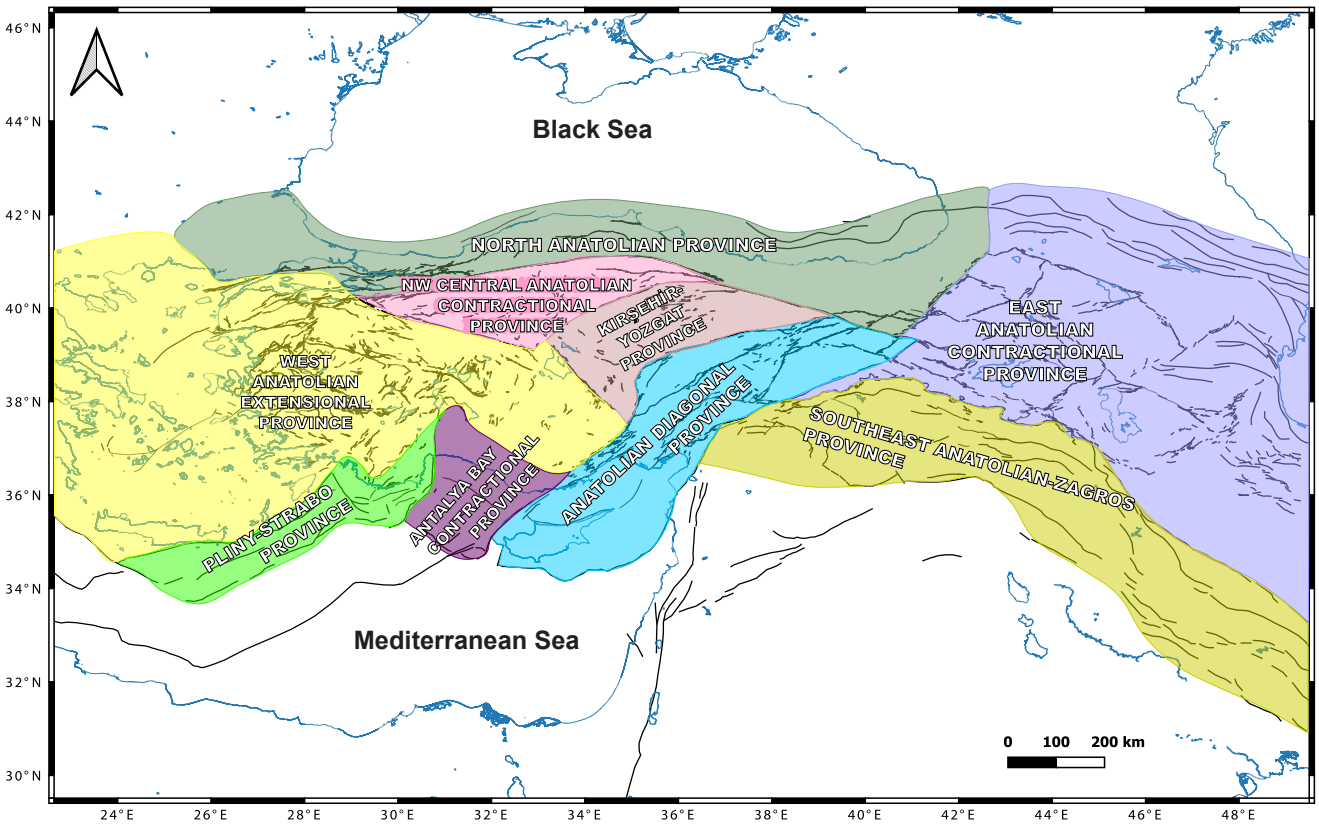

FIGURE 9. Neotectonic provinces of Turkey after taking into account newly introduced structures.

contractional slip rates for the Eldivan-Elmadağ Pinched Crustal Wedge (Esat *et al.*, 2021).

The NAFZ bifurcates in the Bolu plain. The northern branch cuts through the Bolu plain and provides a connection between the main course of NAFZ and the northern border of Almacık block (Seyitoğlu *et al.*, 2015b). In our block modelling the main branch of NAFZ between Yeniçağa and north of Ilgaz provides right-lateral slip rate [-23.7±0.9 (4.3±0.9)] (Figs. 4; 8B). The overall slip rates in the middle branch at the south of Almacık block also indicate right-lateral slip rate [-30.0±7.5 (-7.7±6.8) and -30.7±5.3 (-12.9±7.2)], but the northern branch at the north of Almacık block have dominant contractional slip rate (Fig. 8B). The middle branch of NAFZ has incompatible results with its tectonic character (Fig. 8C). The southern branch of NAFZ gives statistically insignificant results around Mudurnu. However, the block boundaries in Yenişehir [-5.2±2.3 (3.8±2.3)mm/yr], Bayırköy [-4.6±2.2 (2.6±2.3) mm/yr] and northeast of Vezirhan [-4.7±2.3 (0.9±2.2)mm/yr] provide right-lateral slip rates (Figs. 4; 8B). Relatively local block modelling of Seyitoğlu *et al.* (2016), however, provides more reasonable slip rates for the northern, middle, and southern branches of the NAFZ in the Marmara region where the southern branch is determined as a second important branch of the NAFZ after the northern branch.

The continuation of southern branch of the NAFZ in western Turkey (Seyitoğlu *et al.*, 2022b) is unsuccessfully represented in our block modelling, probably due to the en echelon nature of fault segments in this area. Only three block boundaries, around Susurluk and İzmir, provide right-lateral slip rates ranging between -19.1±3.1mm/yr and -9.4±3.2mm/yr (Figs. 4; 8C). The block boundaries representing Alaşehir, Büyük Menderes, Gökova grabens and Denizli-Acıgöl basins, however, provide extensional slip rates which are compatible with the extensional nature of these structures.

CONCLUSIONS

The increasing number of earthquake focal mechanism solutions and determinations of segment distributions by using high-resolution satellite images together with the increasing number of field studies and the examination of active fault traces in the offshore areas have created an opportunity to review the classic view of the Neotectonics of Turkey, established at the beginning of 1980's.

Following issues are new contributions to the neotectonic framework of Turkey.

i) The Southeast Anatolian Wedge is defined between the BZSZ and Sincar Mountain having thrusts and blind thrusts and related asymmetrical folds (Seyitoğlu *et al.*, 2017a) (Fig. 2A, B). Similar structures exist in the foreland of BZSZ in Iraq and Iran, therefore the whole area can be named the Southeast Anatolian-Zagros Province (Fig. 9).

ii) Rhomboidal cells in the Turkish-Iranian Plateau define the position of major shear zones in the region such as the NAFZ, NEAFZ, EAFZ, and SAZFZ. The right-lateral strike-slip NAFZ creates a releasing stepover with the right-lateral SAZFZ where the Kığı, Karlıova, and Muş rhomboidal cells are developed (Seyitoğlu *et al.*, 2018) (Fig. 2A, B). Although new region-wide structures are recognized, they did not change the fact that the entire region is under the north-south contraction. For this reason, the earlier name, the East Anatolian Contractional Province has been preserved (Fig. 9).

iii) The Anatolian Diagonal is a left-lateral strike-slip shear zone demonstrating multiple complex intersections with the right-lateral NAFZ and SAZFZ. i) The Karaca and Kemah-İliç faults of the Anatolian Diagonal connected to the NAFZ west of Erzincan. ii) The intersection of OVF with the NAFZ takes place at the SE of Erzincan. iii) The Ovacık Fault limits the SAZFZ at the WNW of Tunceli. iv) The EAFZ of the Anatolian Diagonal intersects with the SAZFZ in Bingöl (Seyitoğlu *et al.*, 2022a) (Figs. 2A, B; 3).

iv) The offshore continuation of the EDF of the Anatolian Diagonal, the BRF reaches Cyprus Arc at the west of Cyprus. The AKFZ behaves as an en echelon structure between Anatolian Diagonal and PLF/STF faults creating restraining stepovers in the Antalya basin and at the northern margin of the Rhodes basin (Seyitoğlu *et al.*, 2022a) (Figs. 3; 4). The left-lateral shear zone connecting the NAFZ and Cyprus Arc is defined as a new neotectonic area called the Anatolian Diagonal Province (Fig. 9). The Antalya Bay Contractional Province includes Florence Rise and Antalya Thrust. The Antalya-Kekova Fault Zone and Pliny, Strabo faults together with the Fethiye thrust constitute the Pliny-Strabo Province (Fig. 9).

v) The NAFZ, KEFZ and EFZ creates an area affected by the NW-SE contraction (Esat *et al.*, 2021) where the EPCW (Seyitoğlu *et al.*, 2009) and APCW (Esat *et al.*, 2017) pinched crustal wedges and the BBTZ (Ardahanlıoğlu *et al.*, 2020; Seyitoğlu *et al.*, 2017b) are developed (Fig. 5). This area is called the NW Central Anatolian Contractional Province (Fig. 9). The North Anatolian Province and the Kırşehir-Yozgat Province are the neotectonic areas on the north and east respectively (Fig. 9).

vi) The southern branch of the NAFZ are defined from Bolu to Değirmenlik (Milos) island in the Aegean Sea via Mudurnu, Bursa, Balıkesir, Manisa and İzmir (Seyitoğlu *et al.*, 2022b) (Fig. 4). This structure penetrates the West

Anatolian Extensional Province which covers an area from the Aegean Sea to the Tuzgölü Fault Zone (Fig. 9).

vii) A region-wide block modelling in the eastern Mediterranean region provides compatible slip rates for the block boundaries representing the major tectonic elements, such as the NAFZ, NEAFZ, SAZFZ, the margins of Anatolian Diagonal Shear Zone, Cyprus Arc, Florence Rise, Antalya-Kekova Fault Zone, northern margin of Rhodes basin, Pliny-Strabo Fault Zone, and Aegean Arc. However, the block boundaries representing the internal structures of Anatolian plate in central Anatolia provide slip rates incompatible with their tectonic character. While the majority of block boundaries in western Turkey have compatible slip rate results with their well-defined tectonic characters, such as the Alaşehir, Büyük Menderes, and Denizli grabens, the block boundaries representing the southern branch of NAFZ in western Turkey have partly compatible slip rates. As a whole, the block modelling results presented in this paper (Fig. 8A, B, C) may represent a new opportunity to evaluate the major neotectonic provinces in the eastern Mediterranean region (Fig. 9).

REFERENCES

Adıyaman, Ö., Chorowicz, J., Arnaud., O.N., Gündoğdu, M.N., Gourgaud, A., 2001. Late Cenozoic tectonics and volcanism along the North Anatolian Fault: new structural and geochemical data. Tectonophysics, 338, 135-165.

Aksoy, E., İnceöz, M., Koçyiğit, A., 2007. Lake Hazar Basin: A Negative Flower Structure on the East Anatolian Fault System (EAFS), SE Turkey. Turkish Journal of Earth Sciences, 16, 319-338.

Aktaş, G., Robertson, A.H.F., 1984. The Maden complex, SE Turkey: evolution of a Neotethyan active margin. The Geological Society of London, 17 (Special Publications), 375-402.

Aktuğ, B., Doğru, A., Özener, H., Peyret, M., 2015. Slip rates and locking depth variation in the middle and easternmost segments of NAFS. Geophysical Journal International, 202, 2133-2149.

Aktuğ, B., Özener, H., Doğru, A., Sabuncu, A., Turgut, B., Halıcıoğlu, K., Yılmaz, O., Havazlı; E., 2016. Slip rates and seismic potential on the East Anatolian Fault System using an improved GPS velocity field. Journal of Geodynamics, 94-95, 1-12.

Allen, M.B., 2010. Roles of strike-slip faults during continental deformation: examples from the active Arabia - Eurasia collision. The Geological Society of London, 338 (Special Publications), 329-344.

Ardahanlıoğlu, A., Seyitoğlu, G., Esat, K., 2020. The internal structure of Beypazarı Blind Thrust Zone around Çayırhan. Bulletin of the Mineral Research and Exploration, 163, 77-97.

Arpat, E., Şaroğlu, F., 1972. The East Anatolian fault system; thoughts on its development. Bulletin of the Mineral Research and Exploration, 78, 33-39.

Arpat, E., 1977. 1975 Lice depremi. Yeryuvarı ve İnsan, 2/1, 15-27.

Barka, A., Reilinger, R., 1997. Active tectonics of the Eastern Mediterranean region: deduced from GPS, neotectonic and seismicity data. Annali di Geofisica, 40, 587-610.

Barrier, E., Chamot_Rooke, N., Giordano, G., 2004. Geodynamic Maps of the Mediterranean-sheet 1: Tectonics and Kinematics. Commission for the Geological map of the World (CGMW) and UNESCO.

Başokur, A.T., Gökten, E., Seyitoğlu, G., Varol, B., Ulugergerli, E.U., Işık, V., Candansayar, E., Tokgöz, E., 2002. Jeoloji ve jeofizik çalışmalar ışığında 03.02.2002 Çay (Afyon) depremi'nin mekanizması, hasarın nedenleri ve bölgenin deprem etkinliği. Ankara Üniversitesi Mühendislik Fakültesi Yayını, 56pp.

Biddle, K.T., Bultman, T.R., Fairchild, L.R., Yılmaz, P.O., 1987. An approach to structural interpretation of the southeast Turkey fold and thrust belt. Proceedings of 7th Biannual Petroleum Congress of Turkey. The Union of Chambers of Turkish Engineers and Architects (UCTEA), Chamber of Petroleum Engineers, 78-88.

Boray, A., Şaroğlu, F., Emre, Ö., 1985. Isparta büklümü'nün kuzey kesiminde Doğu- Batı daralma için bazı veriler. Jeoloji Mühendisliği Dergisi, 23, 9-20.

Bozkurt, E., 2001. Neotectonics of Turkey-a synthesis. Geodinamica Acta, 14, 3-30.

Bozkurt, E., Park, R.G., 1994. Southern Menderes Massif: an incipient metamorphic core complex in western Anatolia, Turkey. Journal of the Geological Society London, 151, 213-216.

Burchfiel, B.C., Royden, L.H., 1985. North-south extension within the convergent Himalaya region. Geology, 13, 679-682.

Caputo, R., Pavlides, S., 2013. The Greek database of seismogenic sources (GreDaSS), version 2.0.0: A compilation of potential seismogenic sources (Mw>5.5) in the Aegean Region. Websites: http://gredass.unife.it/, DOI: 10.15160/unife/gredass/0200. Last access date: 07.06.2020

Chemenda, A.I., Mattauer, M., Malavieille, J., Bokun, A.N., 1995. A mechanism for syn-collisional rock exhumation and associated normal faulting: Results from physical modeling. Earth and Planetary Science Letters, 132, 225-232.

Crampin, S., Evans, R., 1986. Neotectonics of the Marmara Sea region of Turkey. Journal of the Geological Society London, 143, 343-348.

Çakır, Z., Akoğlu, A.M., 2008. Synthetic aperture radar interferometry observations of the M=6.0 Orta earthquake of June 2000 (NW Turkey): Reactivation of a listric fault. Geochemistry Geophysics Geosystems, 9, Q08009. DOI:10.1029/2008GC002031

Çinku, M.C., Hisarlı, Z.M., Yılmaz, Y., Ülker, B., Kaya, N., Öksüm, E., Orbay, N., Özbey-Üçtaş, Z., 2016. The tectonic history of the Niğde-Kırşehir massif and Taurides since the late Mesozoic: Paleomagnetic evidence for two-phase orogenic curvature in Central Anatolia. Tectonics, 35, 722-811.

Dewey, J.F., Hempton, M.R., Kidd, W.S.F., Şaroğlu, F., Şengör, A.M.C., 1986. Shortening of continental lithosphere: the

neotectonics of Eastern Anatolia a young collision zone. In: Coward, M.P., Ries, A.C. (eds.). Collision Tectonics The Geological Society of London, 19 (Special Publications: Robert M. Shackleton volume), 3-36.

Dewey, J.F., Şengör, A.M.C., 1979. Aegean and surrounding regions: Complex multiplate and continuum tectonics in a convergent zone. Geological Society of America Bulletin, 90, 84-92.

Dirik, K., Göncüoğlu, M.C., 1996. Neotectonic characteristics of central Anatolia. International Geology Review, 38, 807-817.

Duman, T.Y., Emre, Ö., 2013. The East Anatolian Fault: geometry, segmentation and jog characteristics. The Geological Society of London, 372 (Special Publications), 495-529.

Ekström, G., Nettles, M., Dziewonski, A.M., 2012. The global CMT project 2004-2010: Centroid-moment tensors for 13,017 earthquakes. Physics of the Earth and Planetary Interiors, 200-201, 1-9.

Elitez, İ., Yaltırak, C., Aktuğ, B., 2016. Extensional and compressional regime driven left-lateral shear in southwestern Anatolia (eastern Mediterranean): The Burdur-Fethiye Shear Zone. Tectonophysics, 688, 26-35.

Emre, T., Sözbilir, H., 1997. Field evidence for metamorphic core complex, detachment faulting and accomodation faults in the Gediz and Büyük Menderes grabens, western Anatolia. In: Pişkin, Ö., Ergün, M., Savaşçın, M.Y., Tarcan, G. (eds.). Proceedings of the International Earth Sciences Colloquium on the Aegean region (IESCA), 1, 74-93.

Emre, Ö., Duman, T.Y., Doğan, A., Özalp, S., Tokay, F., Kuşçu, İ., 2003. Surface faulting associated with the Sultandağı earthquake (Mw 6.5) of 3 February 2002, southwestern Turkey. Seismological Research Letters, 74, 382-392.

Emre, Ö., Duman, T., Özalp, S., Elmacı, H., Olgun, Ş., Şaroğlu, F., 2013. Active fault map of Turkey with and explanatory text. General Directorate of Mineral Research and Exploration, 30 (Special Publication Series), 89pp.

Emre, Ö., Duman, T.Y., Özalp, S., Şaroğlu, F., Olgun, Ş., Elmacı, H., Çan, T., 2018. Active fault database of Turkey. Bulletin of Earthquake Engineering, 16, 3229-3275.

Esat, K., Çıvgın, B., Kaypak, B., Işık, V., Ecevitoğlu, B., Seyitoğlu, G., 2014. The 2005-2007 Bala (Ankara, Central Turkey) earthquakes: a case study for strike-slip fault terminations. Geologica Acta, 12(1), 71-85.

Esat, K., Kaypak, B., Işık, V., Ecevitoğlu, B., Seyitoğlu, G., 2016. The Ilıca branch of the southeastern Eskişehir Fault Zone: an active right-lateral strike-slip structure in central Anatolia, Turkey. Bulletin of the Mineral Research and Exploration, 152, 25-37.

Esat, K,, Seyitoğlu, G., Ecevitoğlu, B., Kaypak, B., 2017. Abdüsselam Kıstırılmış Tektonik Kaması: KB Orta Anadolu'da daralma rejimiyle ilişkili bir Geç Senozoyik yapısı [Abdüsselam Pinched Crustal Wedge: A Late Cenozoic structure related to the contractional regime in the NW Central Anatolia]. Yerbilimleri-Bulletin for Earth Sciences, 38, 33-56.

Esat, K., Seyitoğlu, G., Kaypak, B., Koca-Çıvgın, B., Özdemirli-Esat, T., 2020. What do we learn from the recent seismic events about the nature of Tuzgölü Fault Zone? Seismotectonics of the Tuzgölü Fault Zone under the light of 2005-2007 Bala (M=5.3; 5.4), 2020.07.12 (M=3.5) Şereflikoçhisar and 2020.09.20 (M=5.3) Obruk earthquakes. Researchgate Technical Report, 6pp. DOI: 10.13140/RG.2.2.28730.41920

Esat, K., Seyitoğlu, G., Aktuğ, B., Kaypak, B., Ecevitoğlu, B., 2021. The Northwest Central Anatolian Contractional Area: a neotectonic deformation zone bounded by major strike-slip fault zones in the Anatolian Plate. Tectonophysics, 805, 228776. DOI: 10.1016/j.tecto.2021.228776

Fossen, H., 2000. Extensional tectonics in the Caledonides: Synorogenic or postorogenic? Tectonics, 19, 213-224.

Hall, R., 1976. Ophiolite emplacement and the evolution of the Taurus suture zone, southeast Turkey. Geological Society of America Bulletin, 87, 1078-1088.

Hall, J., Aksu, A.E., Elitez, İ., Yaltırak, C., Çiftçi, G., 2014. The Fethiye-Burdur Fault Zone: A component of upper plate extension of the subduction transform edge propagator fault linking Hellenic and Cyprus Arcs, Eastern Mediterranean. Tectonophysics, 635, 80-99.

Hempton, M.R., 1985. Structure and deformation history of the Bitlis suture near Lake Hazar, southeastern Turkey. Geological Society of America Bulletin, 96, 233-243.

Herece, E., 2008. Atlas of East Anatolian Fault. Ankara, Turkey. General Directorate of Mineral Research and Exploration, 13 (Special Publication Series), 359pp. ISBN: 978-605-4075-12-6

Howell, A., Jackson, J., Copley, A., McKenzie, D., Nissen, E., 2017. Subduction and vertical coastal motions in the eastern Mediterranean. Geophysical Journal International, 211, 593-620.

Işık, V., Tekeli, O., 2001. Late orogenic crustal extension in the northern Menderes massif (western Turkey): Evidences for metamorphic core complex formation. International Journal of Earth Sciences, 89, 757-765.

Jackson, J., McKenzie, D., 1984. Active tectonics of the Alpine-Himalayan Belt between western Turkey and Pakistan. Geophysical Journal of the Royal Astronomical Society, 77, 185-264.

Jackson, J., 1992. Partitioning of strike-slip and convergent motion between Eurasia and Arabia in eastern Turkey and the Caucasus. Journal of Geophysical Research, 97, 12.471-12.479.

Kamacı, Ö., Altunkaynak, Ş., 2019. Cooling and deformation history of the Çataldağ metamorphic core complex (NW Turkey). Journal of Asian Earth Sciences, 172, 279-291.

Kaya, S., Esat, K., Işık, V., Kaypak, B., Uyar, A.G., Seyitoğlu, G., 2014. Geological and geophysical observations on the tectonic features of western part of the Afyon-Akşehir graben: a contribution to the arguments on the two-stage extension model. Yerbilimleri-Bulletin for Earth Sciences, 35, 1-16.

Kaymakçı, N., Özçelik, Y., White, H.S., Van Dijk, P.M., 2001. Neogene tectonic development of the Çankırı Basin (central Anatolia, Türkiye). Turkish Association of Petroleum Geologists Bulletin (TAPG), 13, 27-56.

Kaymakçı, N., Langereis, C., Özkaptan, M., Özacar, A.A., Gülyüz, E., Uzel, B., Sözbilir, H., 2018. Paleomagnetic evidence for upper plate response to a STEP fault, SW Anatolia. Earth and Planetary Science Letters, 498, 101-115.

Ketin, İ., 1948. Uber die tektonisch-mechanischen Folgerungen aus den grossen anatolischen Erdbeden des letzten Dozennimus. Geologische Rundschau, 36, 77-83.

Koçyiğit, A., Beyhan, A., 1998. A new intracontinental transcurrent structure: the Central Anatolian Fault Zone, Turkey. Tectonophysics, 284, 317-336.

Koçyiğit, A., Ünay, E., Saraç, G., 2000. Episodic graben formation and extensional neotectonic regime in west central Anatolia and the Isparta Angle: a case study in the Akşehir-Afyon graben, Turkey. In: Bozkurt, E., Winchester, J.A., Piper, J.D.A., (eds.). Tectonics and Magmatism in Turkey and the Surrounding Area. The Geological Society of London, 173 (Special Publications), 405-421.

Koçyiğit, A., Rojay, B., Cihan, M., Özacar, A., 2001. The June 6, 2000, Orta (Çankırı, Turkey) Earthquake: Sourced from a new antithetic sinistral strike-slip structure of the North Anatolian Fault System, the Dodurga Fault Zone. Turkish Journal of Earth Sciences, 10, 69-82.

Koçyiğit, A., Özacar, A., 2003. Extensional neotectonics regime through the NE edge of the outher Isparta angle, SW Turkey: New field and seismic data. Turkish Journal of Earth Sciences, 12, 67-90.

Kreemer, C., Blewitt, G., Klein, E.C., 2014. A geodetic plate motion and Global Strain Rate Model. Geochemistry Geophysics Geosystems, 15, 3849-3889.

Krystopowicz, N.J., Schoenbohm, L.M., Rimando, J., Brocard, G., Rojay, B., 2020. Tectonic geomorphology and Plio-Quaternary structural evolution of the Tuzgölü Fault Zone, Turkey: Implications for deformation in the interior of the Central Anatolian Plateau. Geosphere, 16, 18pp. DOI: 10.1130/GEOS02175.1

Kurt, F.S., Işık, V., Seyitoğlu, G., 2010. Alternative Cenozoic exhumation history of the Kazdağ core complex, western Turkey. Tectonic Crossroads: Evolving orogens of Eurasia-Africa-Arabia. Ankara, Abstracts with programs 36-3, 70pp.

Kürçer, A., Gökten, Y.E., 2014. Neotectonic period characteristics, seismicity, geometry and segmentation of the Tuz Gölü Fault Zone. Bulletin of the Mineral Research and Exploration, 149,19-68.

Lister, G.S., Banga, G., Feensta, A., 1984. Metamorphic core complexes of Cordilleran type in the Cyclades, Aegean Sea, Greece. Geology, 12, 221-225.

Mansfield, S,L., 2005. Neogene tectonic and sedimentary evolution of the outer Cilicia basin, eastern Mediterranean Sea. MSc thesis. Memorial University of Newfoundland, 978-0-494-19380-8.

Matsu'ura, M., Jackson, D.D., Cheng, A., 1986. Dislocation model for aseismic crustal deformation at Hollister, California. Journal of Geophysical Research, 91, 2661-2674.

McCaffrey, R., 2002. Crustal block rotations and plate coupling. In: Stein, S., Freymueller, J.T. (eds.). Plate Boundary Zones. American Geophysical Union, Geodynamics Series, 30, 101-122. DOI: 10.1029/030GD06

McKenzie, D.P., 1972. Active tectonics of the Mediterranean region. Geophysical Journal of the Royal Astronomical Society, 30, 109-185.

Ocakoğlu, N., Demirbağ, E., Kuşçu, İ., 2005. Neotectonic structures in İzmir Gulf and surrounding regions (western Turkey): Evidences of strike-slip faulting with compression in the Aegean extensional regime. Marine Geology, 219, 155-171.

Okada, Y., 1985. Surface deformation due to shear and tensile faults in a half-space. Bulletin of the Seismological Society of America, 75, 1135-1154.

Özsayın, E., Çiner, A., Rojay, F.B., Dirik, R.K., Melnick, D., Fernandez-Blanco, D., Bertotti, G., Schildgen, T.F., Garcin, Y., Strecker, M.R., Sudo, M., 2013. Plio-Quaternary extensional tectonics of the Central Anatolian Plateau: a case study from the Tuz Gölü Basin, Turkey. Turkish Journal of Earth Sciences, 22, 691-714.

Perinçek, D., Günay, Y., Kozlu, H., 1987. New observations on strike-slip faults in east and southeast Anatolia. Proceedings of 7th Biannual Petroleum Congress of Turkey. Union of Chambers of Turkish Engineers and Architects (UCTEA), Chamber of Petroleum Engineers, 89-103.

Reilinger, R., McClusky, S., Vernant, P., Lawrence, S., Ergintav, S., Çakmak, R., Özener, H., Kadirov, F., Guliev, I., Stepanyan, R., Nadariya, M., Hahubia, G., Mahmoud, S., Sakr, K., ArRajehi, A., Paradissis, D., Al-Aydrus, A., Prilepin, M., Guseva, T., Evren, E., Dmitrotsa, A., Filikov, S.V., Gomez, F., Al-Ghazzi, R., Karam, G., 2006. GPS constraints on continental deformation in the Africa - Arabia-Eurasia continental collision zone and implications for the dynamics of plate interactions. Journal of Geophysical Research, 111, B05411. DOI: 10.1029/2005JB004051

Ring, U., Laws, S., Bernet, M., 1999. Structural analysis of a complex nappe sequence and late-orogenic basins from the Aegean Island of Samos, Greece. Journal of Structural Geology, 21, 1575-1601.

Ring, U., Johnson, C., Hetzel, R., Gessner, K., 2003. Tectonic denudation of a Late Cretaceous-Tertiary collisional belt-regionally symmetric cooling patterns and their relation to extensional faults in the Anatolide belt of western Turkey. Geological Magazine, 140, 1-21.

Ring, U., Glodny, J., 2010. No need for lithospheric extension for exhuming (U)HP rocks by normal faulting. Journal of the Geological Society London, 167, 225-228.

Rojay, B., Karaca, A., 2008. Post-Miocene deformation in the south of the Galatean volcanic province, NW of central Anatolia (Turkey). Turkish Journal of Earth Sciences, 17, 653-672.

Seyitoğlu, G., Scott, B.C., 1991. Late Cenozoic crustal extension and basin formation in west Turkey. Geological Magazine, 128, 155-166.

Seyitoğlu, G., Scott, B.C., 1992. The age of the Büyük Menderes graben (west Turkey) and its tectonic implications. Geological Magazine, 129, 239-242.

Seyitoğlu, G., Scott, B.C., 1996a. Age of Alaşehir graben (west Turkey) and its tectonic implications. Geological Journal, 31, 1-11.

Seyitoğlu, G., Scott, B.C., 1996b. The cause of N-S extensional tectonics in western Turkey: Tectonic escape vs Back-arc spreading vs Orogenic collapse. Journal of Geodynamics, 22, 145-153.

Seyitoğlu, G., Kazancı, N., Karadenizli, L., Şen, Ş., Varol, B., Karabıyıkoğlu, T., 2000. Rockfall avalanche deposits associated with normal faulting in the NW of Çankırı basin: implications for the post-collisional tectonic evolution of the Neo-Tethyan suture zone. Terra Nova, 12, 245-251.

Seyitoğlu, G., Işık, V., Çemen, I., 2004a. Complete Tertiary exhumation history of the Menderes massif, western Turkey: an alternative working hypothesis. Terra Nova, 16, 358-364.

Seyitoğlu, G., Kazancı, N., Karadenizli, L., Şen, Ş., Varol, B., Saraç, G., 2004b. Neogene tectono-sedimentary development of western margin of Çankırı basin, central Turkey: reply to the comment of Kaymakçı 2003. Terra Nova, 16, 163-165.

Seyitoğlu, G., Aktuğ, B., Karadenizli, L., Kaypak, B., Şen, Ş., Kazancı, N., Işık, V., Esat, K., Parlak, O., Varol, B., Saraç, G., İleri, İ., 2009. A Late Pliocene - Quaternary pinched crustal wedge in NW central Anatolia, Turkey: A neotectonic structure accommodating the internal deformation of the Anatolian Plate. Geological Bulletin of Turkey, 52, 121-154.

Seyitoğlu, G., Işık, V., 2015. Late Cenozoic extensional tectonics in western Anatolia: Exhumation of the Menderes core complex and formation of related basins. Bulletin of the Mineral Research and Exploration, 151, 47-106.

Seyitoğlu, G., Ecevitoğlu, B., Kaypak, B., Güney, Y., Tün, M., Esat, K., Avdan, U., Temel, A., Çabuk, A., Telsiz, S., Uyar, Aldaş, G., 2015a. Determining the main strand of the Eskişehir strike-slip fault zone using subsidiary structures and seismicity: a hypothesis tested by seismic reflection studies. Turkish Journal of Earth Sciences, 24, 1-20.

Seyitoğlu, G., Ecevitoğlu, B., Kaypak, B., Esat, K., Çağlayan, A., Gündoğdu, O., Güney, Y., Işık, V., Pekkan, E., Tün, M., Avdan, U., 2015b. A missing-link in the tectonic configuration of the Almacık Block along the North Anatolian Fault Zone (NW Turkey): active faulting in the Bolu plain based on seismic reflection studies. Geophysical Journal International, 201, 1814-1833.

Seyitoğlu, G., Kaypak, B., Aktuğ, B., Gürbüz, E., Esat, K., Gürbüz, A., 2016. A hypothesis for the alternative southern branch of the North Anatolian Fault Zone, Northwest Turkey. Geological Bulletin of Turkey, 59, 115-130.

Seyitoğlu, G., Esat, K., Kaypak, B., 2017a. The neotectonics of southeast Turkey, northern Syria and Iraq: the internal structure of the Southeast Anatolian Wedge and its relationship with the recent earthquakes. Turkish Journal of Earth Sciences, 26, 105-126.

Seyitoğlu, G., Esat, K., Kaypak, B., 2017b. One of the main neotectonic structures in the NW central Anatolia: Beypazarı Blind Thrust Zone and related fault-propagation folds. Bulletin of the Mineral Research and Exploration, 154, 1-14.

Seyitoğlu, G., Esat, K., Kaypak, B., Toori, M., Aktuğ, B., 2018. Internal deformation of the Turkish-Iranian Plateau in the hinterland of Bitlis-Zagros Suture Zone. In: Farzipour, S.A., (ed.). Tectonic and Structural Framework of the Zagros Fold-Thrust Belt. Elsevier, 161-244.

Seyitoğlu, G., Toori, M., Esat, K., Kaypak, B., 2019. Tectonic significance of the thrust parallel-normal faulting in the northern Makran accretionary wedge of Iran and Pakistan. 72nd Geological Congress of Turkey, The Proceedings and Abstract Book, ISBN:978-605-01-1261-0, 967-972.

Seyitoğlu, G., Kaypak, B., Esat, K., Toori, M., 2020. The focal mechanism solution of 2020.10.25 (Mw=4.1) Sancaklı-Bingöl earthquake and an evaluation of the seismicity along the Southeast Anatolian-Zagros Fault Zone. Researchgate Technical Report, 4pp. DOI: 10.13140/RG.2.2.23793.10083

Seyitoğlu, G., Esat, K., 2022. Uludağ extensional metamorphic core complex: preliminary field observations. Bulletin of the Mineral Research and Exploration, DOI:10.19111/bulletinofmre.1029034

Seyitoğlu, G., Tunçel, E., Kaypak, B., Esat, K., Gökkaya, E., 2022a. The Anatolian Diagonal: a broad left-lateral shear zone between the North Anatolian Fault Zone and Aegean/Cyprus arcs. Geological Bulletin of Turkey, 65, 93-116. DOI: 10.25288/tjb.1015537

Seyitoğlu, G., Esat, K., Kaypak, B., Koca, B., 2022b. Seismotectonics of the southern branch of North Anatolian Fault Zone along Bolu, Bursa, and İzmir cities and Değirmenlik (Milos) island in the Aegean Sea. Yerbilimleri-Bulletin for Earth Sciences. DOI: 10.17824/yerbilimleri.948130

Şahbaz, N., Seyitoğlu, G., 2018. The Neotectonics of NE Gaziantep: The Bozova and Halfeti strike- slip faults and their relationships with blind thrusts, Turkey. Bulletin of the Mineral Research and Exploration, 156, 17-40.

Şaroğlu, F., Emre, Ö., Boray, A., 1987. Active faults and seismicity in Turkey. Ankara (Turkey), MTA report Nº 8174, 394pp.

Şaroğlu, F., Emre, Ö., Kuşçu, İ., 1992a. Active Fault Map of Turkey. Ankara (Turkey), General Directorate of Mineral Research and Exploration.

Şaroğlu, F., Emre, Ö., Kuşçu, İ., 1992b. The East Anatolian Fault Zone of Turkey. In: Bucknam, R.C., Hancock, P.L. (eds.). Major active faults of the world. Results of International Geoscience Programme (IGCP) project 206, Annales Tectonicae, IV (supplement), 99-125.

Şengör, A.M.C., 1979. The North Anatolian transform fault: its age, offset and tectonic significance. Journal of the Geological Society London, 136, 269-282.

Şengör, A.M.C., Kidd, W.S.F., 1979. Post-collisional tectonics of the Turkish-Iranian Plateau and a comparison with Tibet. Tectonophysics, 55, 361-376.

Şengör, A.M.C., Yılmaz, Y., 1981. Tethyan evolution of Turkey: A plate tectonic approach. Tectonophysics, 75, 181-241.

Şengör, A.M.C., Görür, N., Şaroğlu, F., 1985. Strike-slip deformation basin formation and sedimentation: Strike-slip faulting and related basin formation in zones of tectonic escape: Turkey as a case study. In: Biddle, K.T., Christie-Blick,

N. (ed.). Strike-slip faulting and basin formation. Society of Economic Paleontologists and Mineralogists, 37 (Special Publication), 227-264.

Şengör, A.M.C., 1987. Cross-faults and differential stretching of hanging walls in regions of low-angle normal faulting: examples from western Turkey. In: Coward, M.P., Dewey, J.F., Hancock, P.L. (eds.). Continental Extensional Tectonics. The Geological Society of London, 28 (Special Publications), 575-589.

Şengör, A.M.C., Özeren, S., Genç, T., Zor, E., 2003. East Anatolian high plateau as a mantle-supported, north-south shortened domal structure. Geophysical Research Letters, 30, 8045. DOI: 10.1029/2003GL017858

Şengör, A.M.C., Özeren, M.S., Keskin, M., Sakınç, M., Özbakır, A.D., Kayan, İ., 2008. Eastern Turkish high plateau as a small Turkic-type orogen: Implications for post-collisional crust-forming processes in Turkic-type orogens Earth-Science Reviews, 90, 1-48.

Tan, O., Tapırdamaz, C., Yörük, A., 2008. The earthquake catalogues for Turkey. Turkish Journal of Earth Sciences, 17, 405-418.

Tatar, O., Piper, J.D.A., Gürsoy, H., 2000. Palaeomagnetic study of the Erciyes sector of the Ecemiş Fault Zone: neotectonic deformation in the southeastern part of the Anatolian Block. In: Bozkurt, E., Winchester, J.A., Piper, J.D.A. (eds.). Tectonics and Magmatism in Turkey and the Surrounding Area. The Geological Society of London, 173 (Special Publication), 423-440.

Taymaz, T., Tan, O., 2001. Source parameters of June 6, 2000 Orta-Çankırı (Mw=6.0) and December 15, 2000 Sultandağ-Akşehir (Mw=6.0) earthquakes obtained from inversion of teleseismic P- and SH-body-waveforms. Symposia on seismotectonics of the north-western Anatolia-Aegean and recent Turkish earthquakes, 96-107.

Taymaz, T., Wright, T., Yolsal, S., Tan, O., Fielding, E., Seyitoğlu, G., 2007. Source characteristics of the 6 June 2000 Orta-Çankırı (central Turkey) earthquake: a synthesis of seismological, geological and geodetic (InSAR) observations, and internal deformation of the Anatolian plate. In: Taymaz, T., Yılmaz, Y., Dilek, Y. (eds.). The Geodynamics of the Aegean and Anatolia. The Geological Society of London, 291 (Special Publication), 259-290.

Topuz, G., Candan, O., Zack, T., Yılmaz, A., 2017. East Anatolian plateau constructed over a continental basement: No evidence for the East Anatolian accretionary complex. Geology, 45, 791-794.

Uzel, B., Sözbilir, H., 2008. A first record of a strike-slip basin in western Anatolia and its tectonic implication: The Cumaovası basin. Turkish Journal of Earth Sciences, 17, 559-591.

Uzel, B., Sözbilir, H., Özkaymak, Ç., Kaymakçı, N., Langereis, C.G., 2013. Structural evidence for strike-slip deformation in the İzmir-Balıkesir transfer zone and consequences for late Cenozoic evolution of western Anatolia (Turkey). Journal of Geodynamics, 65, 94-116.

ten Veen, J.H., Boulton, S.J., Alçiçek, M.C., 2009. From paleotectonics to neotectonics in the Neotethys realm: The importance of kinematic decoupling and inherited structural grain in SW Anatolia (Turkey). Tectonophysics, 473, 261-281.

Yaltırak, C., İşler, E.B., Aksu, A.E, Hiscott, R.N., 2012. Evolution of the Bababurnu Basin and shelf of the Biga Peninsula: Western extension of the middle strand of the North Anatolian Fault Zone, Northeast Aegean Sea, Turkey. Journal of Asian Earth Sciences, 57, 103-119.

Yılmaz, Y., 1993. New evidence and model on the evolution of the southeast Anatolian orogen. Geological Society of America Bulletin, 105, 251-271.

Manuscript received March 2021;
revision accepted March 2022;
published Online April 2022.